Technical Report Number 2

Office of Naval Research Contract Number: N00014-71-A-0339-0001
(Project No. NR 032-529)

entitled

"Characterization of Tissue Ingrowth Into Porous Bioceramics"

Submitted by

S. F. Hulbert, J. J. Klawitter, B. W. Sauer, and J. R. Matthews

Division of Interdisciplinary Studies

College of Engineering

Clemson University

Clemson, South Carolina 29631

May 1, 1972

Submitted To

Material Science Division
Office of Naval Research
Department of the Navy
Arlington, Virginia 22217

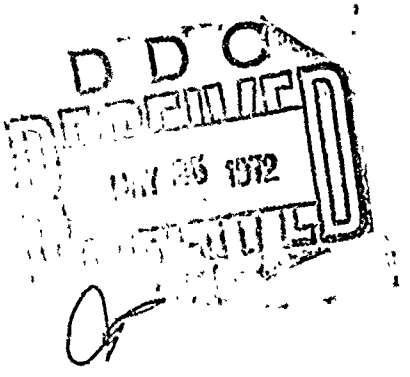

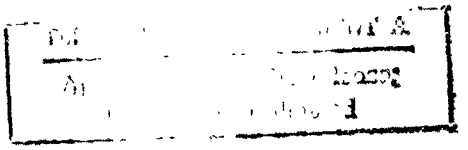

Security Classification

DOCUMENT CONTROL DATA - R & D

Security classification of title, body of abstract and indexing annotation must be entered when the overall report is classified

1 ORIGINATING ACTIVITY (Corporate author)

College of Engineering
Clemson University
Clemson, South Carolina 29631

2a. REPORT SECURITY CLASSIFICATION

Unclassified

2b. GROUP

3 REPORT TITLE

"Characterization of Tissue Ingrowth Into Porous Bioceramics"

4 DESCRIPTIVE NOTES (Type of report and inclusive dates)

Technical Report (No. 2 Covering Period September 1971 to April 1972)

5 AUTHOR(S) (First name, middle initial, last name)

Samuel F. Hulbert, Jerome J. Klawitter, Barry W. Sauer, and Joel R. Matthews

6 REPORT DATE	7a. TOTAL NO. OF PAGES	7b. NO. OF REFS
May 1, 1972	141	102

8a. CONTRACT OR GRANT NO.	9a. ORIGINATOR'S REPORT NUMBER(S)
N00014-71-A-0339-0001	
b. PROJECT NO. NR 032-529	
c.	9b. OTHER REPORT NO(S) (Any other numbers that may be assigned this report)
d.	

10 DISTRIBUTION STATEMENT

Distribution of this document is unlimited

11 SUPPLEMENTARY NOTES	12. SPONSORING MILITARY ACTIVITY
	Office of Naval Research Department of the Navy Washington, D. C. 20360

13 ABSTRACT

A study of the tissue compatibility of the aluminum oxide implant material under different stress conditions in rabbits was performed over 4- and 8-week implantation periods. The specific objectives was to examine endosteal bone ingrowth into aluminum oxide cone-shaped stump plugs in amputated tibiae, while additional pellet-shaped implants in the tibiae and femur of rabbits with amputated and non-amputated limbs were studied to determine: (a) if the degree of loading placed on the amputated limb was sufficient to promote bone activity, (b) the degree of inertness and/or toxicity of the aluminum oxide implants, and (c) a possible cause of bone spurs.

The results of the radiographic, histologic and microradiographic analyses of the in vivo implants demonstrated that there was little mineralized bone ingrowth into the cone-shaped aluminum oxide implants in the amputated tibiae. The study also showed that the aluminum oxide pellet implants in the tibiae and femur of the non-amputated limbs demonstrated excellent mineralized bone ingrowth into surface and internal pores. By comparing these results with the incomplete ingrowth into corresponding pellet implants in the tibiae and femur of amputated limbs, it was determined that a lack of weight bearing and damage to the musculature and vascularity following amputation were interferring with the normal bone activity and therefore bone ingrowth.

Calcium aluminate pellet implants in the tibiae and femora of non-amputated limbs demonstrated less ingrowth than corresponding aluminum oxide implants. The calcium aluminate demonstrated the presence of an osteoid seam. The aluminum oxide implants were completely non-toxic and elicited no inflammatory response. In contrast to the calcium aluminate ceramics, there was little or no osteoid seam separating the aluminum oxide implants and mineralized bone.

14 KEY WORDS	LINK A		LINK B		LINK C	
	ROLE	WT	ROLE	WT	ROLE	WT
Bioceramics						
Kinetics of tissue ingrowth into porous ceramics						
Tissue response to ceramic implants						
Bone grafts						
Orthopedic implants						
Bone segmental replacement						
Implant material characterization						
Implant evaluation						
Aluminum oxide						
Calcium aluminate						
Direct skeletal attachment of artificial limbs						
In vivo testing of implants						
Microangiography						
Microradiography						
Histology						

ABSTRACT

A study was made to determine the feasibility of using porous aluminum oxide for direct skeletal fixation of orthopaedic appliances. The investigation included a material and *in vivo* analysis of the proposed aluminum oxide implant material.

A study of the tissue compatibility of the aluminum oxide implant material under different stress conditions in rabbits was performed over 4- and 8-week implantation periods. The specific objectives was to examine endosteal bone ingrowth into aluminum oxide cone-shaped plugs in amputated tibiae, while additional pellet-shaped implants in the tibiae and femur of rabbits with amputated and non-amputated limbs were studied to determine (a) if the degree of loading placed on the amputated limb was sufficient to promote bone activity, (b) the degree of inertness and/or toxicity of the aluminum oxide implants, and (c) a possible cause of bone spurs.

The results of the radiographic, histologic and microradiographic analyses of the *in vivo* implants demonstrated that there was little mineralized bone ingrowth into the cone-shaped aluminum oxide implants in the amputated tibiae. The study also showed that the aluminum oxide pellet implants in the tibiae and femur of the non-amputated limbs demonstrated excellent mineralized bone ingrowth into surface and internal pores. By comparing these results with the incomplete ingrowth into corresponding pellet implants in the tibiae and femur of amputated limbs, it was determined that a lack of weight bearing

and damage to the musculature and vascularity following amputation were interferring with the normal bone activity and therefore bone ingrowth.

Calcium aluminate pellet implants in the tibiae and femoral of non-amputated limbs demonstrated less ingrowth than corresponding aluminum oxide implants. The calcium aluminate demonstrated the presence of an osteoid seam. The aluminum oxide implants were completely non-toxic and elicited no inflammatory response. In contrast to the calcium aluminate ceramics, there was little or no osteoid seam separating the aluminum oxide implants and mineralized bone.

Angiographs and radiographs of the amputated tibiae demonstrated that bone spurs were present and that they originated at the side of the periosteal damage. Their cause was believed to be associated with an increase in the vascularity of the adjacent tissues.

TABLE OF CONTENTS

Chapter Page

LIST OF TABLES

LIST OF FIGURES

Figure | Page

Figure Page

CHAPTER I

INTRODUCTION

The earliest known use of an artificial limb dates back to the time of Herodotus whose writings in "History" tell of a Persian soldier, Hegesistratus of Elis, who, after being forced to amputate part of his foot as the only means of escape from the Spartans, replaced it later with a wooden one (54, 100). This early attempt at replacement of a lost limb may be thought of as the beginning of the field now referred to as Limb Prosthetics.

Through the years improvements have been made in the surgical procedure and in the construction, attachment, and control of artificial limbs which have enabled orthopedists and prosthetists to, in most cases, rehabilitate the amputee to a condition which permits him to follow his professional and social interests with varying limitations.

The period immediately following amputation is critical to the amputee for he must prepare psychologically and physically for an artificial limb. The current philosophy on post-surgical care is that the immediate application of a temporary prosthesis while the patient is still anesthized will significantly reduce the occurrance of muscle and skin contracture and edema in the stump. It will also greatly increase comfort when the permanent prosthesis is fitted (98). The sockets of the prostheses worn today are, in most cases, fabricated from a porous plastic laminate which op-

timizes strength, weight, and comfort (33, 39). To distribute the load evenly, an impression is made of the stump prior to fitting the permanent prosthesis and the plastic socket is molded to correspond to the stump. The overall shape of the prosthesis as well as the presence of attachments such as an artificial hand will depend on the location of the amputation.

The prosthesis is retained in place with either a leather corset or harness, again, depending on the location. In cases where the length and shape of the stump are suitable, as with the Syme amputation, a suction socket is utilized.

The control of most of the lower extremity prostheses is by muscular contractions in the remaining stump as in the case of below-knee amputations, or by the use of a constant-friction knee unit--and in some cases a hydraulic unit--for the hip disarticulation and above-knee amputations. Upper extremity prostheses are controlled by muscles in the remaining stump, or body movements--such as curling of the shoulders--which activate control cables (33). See Figure 1.

The techniques described for rehabilitation of the amputee have a number of limitations and shortcomings which are inherent in this type of indirect attachment of an artificial limb to the skeletal system. There is a very significant loss of energy along with the poor cosmetic appearance associated with prostheses which are activated by body movements, such as curling the shoulders. The fact that the body has a limited number of control sites capable

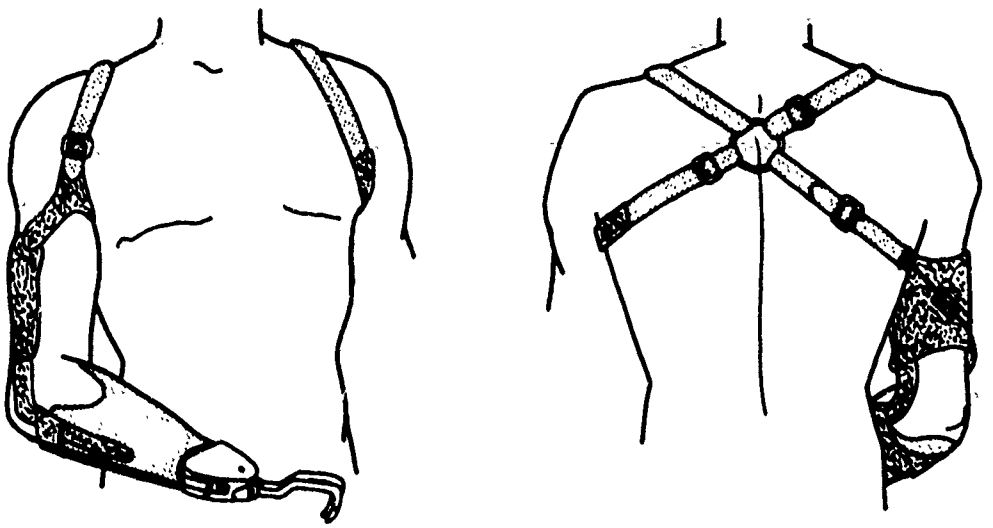

(a) (b)

Figure 1. Below-elbow amputation with typical limb prosthesis; (a) anterior, (b) posterior.

of operating these mechanical controls often causes the amputee to have to sacrifice axes of motion. Further power loss takes place where forces are transmitted from the skeletal system through muscle and skin to the prosthesis' housing. Many prostheses, such as those for the hip and shoulder disarticulations, must be held in place by a system of support straps. These are inefficient, uncomfortable, and cosmetically undesireable.

A further intrinsic limitation in today's prostheses is a loss of feedback from the artificial limb. Control of a normal extremities' actions comes from a continuous force, velocity, and acceleration feedback to the brain. Following amputation, control of upper limb prostheses is derived from visual feedback; this greatly limits the efficiency of motion for the amputee.

Many further complications critical to the rehabilitation of the amputee are traced to abnormal conditions which arise in the stump. These may be in the form of an abnormal bone growth, edema, muscle and skin contractures, or disuse osteoporosis.

Abnormal bone growths in the form of bone spurs and distal bone overgrowth will cause discomfort and, in some cases, necessitate surgical revision of the stump. A bone spur is a periosteal proliferation directed away from the axis of the long bone, which, if present, causes physical irritation of the soft tissues adjacent to it. Distal bone overgrowth, which occurs only in juvenile amputees, is associated with a lengthening of the amputated bone along its longitudinal axis. The soft tissues stretch as the bone

continues to lengthen, causing ulceration; in extreme cases, the bone protrudes through the skin leaving a path open to infection. Attempts have been made to retard or stop distal bone overgrowth by applying a mushroomed shaped, silicone rubber plug to the bone tip (25, 88, 89). Early results indicate that bone overgrowth is reduced and that stumps are capable of tolerating increased end-bearing loads (89).

Improper fitting of the plastic socket to the stump will create an uneven force distribution which may cause body fluid accumulation, edema, and skin ulceration (33, 100). If unchecked, the amputee will soon be unable to wear a prosthesis. Muscle and skin contractures are caused by inactivity of the tissues and a diminished blood supply (65, 79, 100). They are usually eliminated or reduced by proper post-surgical care and good surgical technique. Stumps which are inactive because the prosthesis is not worn or because the limb is immobilized, will show signs of disuse osteoporosis (45, 46, 84). This condition, which is characterized by diminished bone formation and an overall thinning of the cortical bone, can be alleviated by resumption of activity.

See Appendix I for a more thorough discussion of stump complications.

CHAPTER II

REVIEW OF LITERATURE

Direct skeletal attachment of an artificial limb to a bone stump would eliminate many of the complications which prevent the complete rehabilitation of most amputees. Foremost among these would be the deletion of the plastic socket and support straps which are associated with much of the pain, discomfort, poor cosmetic appearance, and the loss of energy during force transmittal.

Direct Skeletal Attachment

Mechanical or chemical bonding may be used to obtain direct skeletal attachment of a high strength metal or ceramic to cortical bone. The first of these, mechanical attachment, is divided into 4 groups; screw, impaction, acrylic cement, and interlocking bonds.

The early attempts at fixation to the skeletal system were made by screwing the desired prosthesis into the surface of the cortical bone (17, 18, 37). Although often successful for short term fixation, the corrosion of 316L stainless steel multicomponent devices and the high stress concentrations associated with a screw-plate design caused the prostheses to fail mechanically, or resulted in significant pressure necrosis to render the screws useless, or the emission of toxic corrosion products elicited a foreign body reaction.

With the introduction of cobalt-chrome alloys (Vitallium) into widespread use, the 1-piece impaction devices showed greater promise.

Vitallium Moore (40, 70, 73, 76, 82, 94) and Thompson (7, 14, 19, 28, 70, 75, 94) prostheses were used for hip arthroplasty with varying success. The rectangular stem was designed to reduce stress concentrations on the endosteal surface and to resist torsional loads, while the collar was devised to support tensile and compressive loads. However, in many cases, bone necrosis was evident around the areas of contact with bone, resulting in loosening and migration of the prostheses.

Hall (34) experimented with stainless steel intramedullary pins impacted into the tibiae of 6 laboratory canines. Attached to the dostal end of each implant was a polypropylene cone with a Nylon velour surface attached, which he hoped would promote tissue adherance. All failed prematurely because the canines chewed the skin interfaces, there was contraction of the skin from the distal end of the stump, or due to inadequate post-operative care. A later attempt was made to save function on a traumatically amputated hind leg on a young thoroughbred horse. A Vitallium intramedullary rod was constructed with a velour covered polypropylene cone similar to the stainless steel implants. This prosthesis functioned successfully for 9 months.

It was the early work by Kiaer and Haboush (32), which showed that plastic prostheses could be bonded with methacrylate to the cancellous bone in the proximal region of the femur, that gave Charnley (13, 14, 15, 16) the idea to use methacrylate for fixation of both a Thompson stainless steel and a Moore Vitallium prostheses

to the cortical bone of the femoral shaft. His procedure was to first fill the medullary cavity with premixed methacrylate powder, liquid, and catylyst, and then to insert and seat the prosthesis' stem firmly within it. Although during the 15 minute hardening time the methacrylate reached a maximum temperature of 80 degrees Centigrade, it was Charnley's opinion that the metal portion of the stem would absorb most of the heat to prevent tissue damage. However, later studies demonstrated that the opposing layers of bone were being destroyed but that it appeared to have little effect on the success of the prostheses.

Charnley's work indicated that there was no abnormal bone reaction to the acrylic (13), no failures of the acrylic, and little or no change in the femur thickness or texture following hip arthroplasty with a methacrylate bonded prosthesis. In cases where there has been tissue reaction reported, it has been associated with fine pieces of methacrylate which abraided away during mechanical movement of an acrylic acetabulum, not from the intramedullary bond. From a study of 2,000 hip arthroplastics, Charnley has reported a 98 percent success rate with the failures being caused by surgical infection.

Charnley demonstrated the strength of the methacrylate bond by attempting to forcibly remove implants from human femurs post-mortem. In the case of the Thompson prosthesis, the stem came out leaving the acrylic. With the Moore prosthesis, a chisel had to be used to separate the bone from the acrylic.

The fourth group of mechanically bonded prostheses are the porous materials which become physically interlocked with the bone.

It was the opinion of Ross and Smith (80) that porous ceramics possessed all of the desirable traits for a permanent skeletally fixed prosthesis, except that they are extremely brittle. To overcome this, a two phase composite, Cerosium, was developed using a 46 percent porous ceramic with an average pore size of 18 to 25 microns which was impregnated with a cross linked epoxy. The resulting Modulus of Elasticity was the same as bone, thus eliminating localized stresses at the bone-prosthesis interface when loading was applied (85). Four-month implant studies in the femora of dogs demonstrated firm mechanical bonding by new bone adjacent to the Cerosium, although a thin fibrous layer did separate the implant from the calcified bone (80, 85). Cerosium was tested over a 20 month period for toxicity in rats and over a 2 year period for carcinogenicity in mice. Both tests showed negative responses (80).

Mooney (69) reported the use of a Cerosium prosthesis in the humerus of a human triple amputee. The skeletal attachment developed to a point at which a 60 pound weight could be supported. It was only after recurrent infection at the Dacron velour skin interface, that the 9 month old implant had to be removed (69). After later studies indicated that the epoxy was not completely non-toxic, Mooney continued his in vivo testing with glassy carbon osseous implants. These showed ingrowth into the grooves and splines

of the prostheses' stems. The test demonstrated an interfacial shear stress strength of 2,000 pounds per square inch (63). Attempts are now being made by Mooney to study aluminum oxide and high strength graphite implants coated with a glassy carbon to determine their desirability as a means of permanent skeletal fixation.

Klawitter (55) and Talbert (91) implanted porous calcium aluminate pellets into the diaphyses of canine femora for periods of from 4 to 22 weeks in an attempt to determine optimum pore size and the material toxicity. Their results demonstrated that a minimum interconnection pore size of 100 microns was necessary for mineralized bone ingrowth and that an osteoid seam approximately 50 microns wide was present between the implants and the mir alized bone suggesting that the calcium aluminate was hydrating. Although there were no toxic reactions towards the implants, the hydration did prevent complete calcification of the infiltrating tissue.

Further work at Clemson University by Bowman (10) demonstrated excellent infiltration of mineralized bone into porous procelain and titanium pellets in canine femora following 6 and 12 week implantation periods. It was also noted that calcified bone was in direct apposition to both of the ceramics.

With the apparent success of the porous ceramic materials for obtaining interfacial bonding between bone and prosthesis, the idea of using porous metals was brought to interest (41). Titanium was chosen because of its ability to form a strong protective oxide

coating, because it can easily be formed, and because of its reported tissue compatibility (8, 29). Two types of material forming techniques are being studied.

Galante et al. (29) prepared samples by "molding and sintering short metal fibers" of titanium. This technique had the advantage (over using powders) of not being dependent on the material's particle size which would limit the pore size and the number of pore interconnections. This method also increases strength because failure must be from a progressive rupture of multiple bonds between tween fibers (29). The implants were formed from a solid inner titanium rod surrounded by the porous titanium which was fabricated by compressing fine fibers in a die punch. Implants of 45 and 65 percent porosity which were removed from the trochantric and suprachondylar region of rabbit femora after 3 weeks demonstrated partial infiltration of calcified bone within the titanium fibers. Implants removed after 3 months demonstrated complete calcified bone penetration. For an unknown reason, there appeared to be better ingrowth into the 45 percent porous specimens than the 65 percent specimens. A better understanding of this material is dependent upon further long range tissue compatibility and mechanical <u>in vivo</u> testing of the proposed hip prostheses.

Westerman (99) reported a powder metallurgy technique for the forming of porous titanium implants. After MgO and titanium are pressed and fired, the MgO is leached out to form the porous structure. The surface is then pacified with the formation of a protec-

ive titanium oxide coating. By affixing this type of porous outer laminate to a solid core implant, high strength intramedullary fixation would be feasible. A biocompatibility study conducted by Clarke of the University of Washington indicates excellent tissue compatibility and ingrowth. Although this technique is quite promising biologically, there are still technical difficulties encountered when trying to retain strength with porosity.

The field of chemical bonding prosthesis to the musculo-skeletal system received little or no attention until Hench (37) began experimentation with mixing calcium and phosphate ions in a glass-ceramic implant. It was his theory that a material could be developed which, when bonded to the metal prosthesis' stem, could be used for permanent intramedullary fixation. Samples made of a SiO_2-P_2O_5-CaO-Na_2O composite with calcium and phosphate ions precipitating out in a 5 to 1 ratio were placed in the cortical bone of rat femora. Studies made with a scanning electron microscope of the interface between the implant and the bone showed bone in direct apposition to the implant after 6 weeks with no excessive inflammation present. This suggested that perhaps the PO_4^{---} is favorably effecting the collagen formation and mineralization.

CHAPTER III

SELECTION OF PROBLEM

The many attempts at obtaining direct permanent skeletal attachment of an artificial limb have failed prematurely because of infection at the transcutaneous attachment or because of the lack of suitable bonding of the prosthesis to the cortical bone of the amputated limb. Solving the problem of direct skeletal attachment will depend upon the development of a material with the following characteristics: (a) it must not initiate any adverse change or reaction in the body, (b) it must be sufficiently durable and resistant to fatigue to withstand forces normally encountered by bone, (c) it must provide a means for permanent high strength skeletal attachment, and (d) it must be easily fabricated, formed, and sterilized for implantation without loss of properties.

A research program was organized by the authors with the objective of studying the feasibility of suing porous aluminum oxide as a means of direct skeletal fixation for a permanently attached artificial limb.

The study involved a characterization of the mechanical properties and microstructure of the aluminum oxide in conjunction with an in vivo testing to determine tissue compatibility under different stress conditions.

CHAPTER IV

EXPERIMENTAL PROCEDURE

Introduction

To study the feasibility of using porous aluminum oxide as a means of skeletal fixation for a permanently attached artificial limb, the authors chose to analyze the specific case of endosteal ingrowth into a stump plug in an amputated tibia. The lack of a skin interface was preferred because it eliminated the variable of possible infection caused by the lack of a suitable transcutaneous seal.

A further series of implants were made to characterize the other dependent variables which the authors felt would affect the success of the endosteal implants. These included the determination of whether or not the leg was stressed sufficiently to promote normal bone activity, inertness and toxicity of the material, and finally, a possible cause of bone spurs.

Type and Purpose of Implants

Four groups of implants were made to provide the desired data:

CONE IMPLANT GROUP - The left hind leg of each animal was amputated at the tibia-fibula junction, and a cone shaped aluminum oxide implant inserted into the medullary cavity. A second aluminum oxide implant in the shape of a pellet was inserted perpendicularly into the lateral surface of the middle of the dia-

physis of the femur The right leg received no implants.

PELLET IMPLANT GROUP - The left hind leg was amputated at the tibia-fibula junction and an aluminum oxide pellet inserted perpendicularly into the medial surface of the tibia and approximately 25 millimeters from the site of amputation. An aluminum oxide pellet was inserted into the femur as previously described.

BILATERAL IMPLANT GROUP - Aluminum oxide pellets were inserted into the tibia and femur of the right hind limb of each animal and calcium aluminate pellets were likewise inserted into the left tibia and femur, as previously described. No amputation was performed.

PERIOSTEAL SCRAPE GROUP - The left hind leg was amputated approximately 25 millimeters below the tibia-fibula junction and the periosteum removed up to the junction.

Implantations were made in 6 animals for each of the CONE, PELLET, and BILATERAL IMPLANT GROUPS. Of the 6 animals in each group, 3 were implanted for 4 weeks and 3 for 8 weeks. In the PERIOSTEAL SCRAPE GROUP, 4 animals were used for a period of 4 weeks each. The total number of animals used was 22.

These implants were analyzed to obtain the following information:

(a) the type and depth of bone ingrowth into the endosteal implants in the tibiae of the CONE IMPLANT GROUP.

(b) to determine if the animal utilized the leg sufficiently to provide the necessary stress for normal bone activity, the aluminum oxide pellet implants in the tibiae and femora of the amputated limbs of the PELLET IMPLANT GROUP were compared to corresponding aluminum oxide pellets in the non-amputated, normally stressed limbs of the BILATERAL IMPLANT GROUP.

(c) material inertness and toxicity were analyzed by performing a histological study of all aluminum oxide implants, and from a comparison study of calcium aluminate and corresponding aluminum oxide pellet implants from the BILATERAL IMPLANT GROUP.

(d) one theory has associated the formation of bone spurs with the presence of a blood hematoma at the site of the amputation, while another explained this as an overgrowth of the periosteum following surgical irritation. By surgically stripping the periosteum from the tip of the bone following amputation, PERIOSTEAL SCRAPE GROUP, results would indicate whether the spurs formed at the site of the hematoma or at the area of damaged periosteum.

Material Characterization

Material Selection

The results of studies by Klawitter (55) and Talbert (91) demonstrated that mineralized bone had infiltrated into surface

pores of calcium aluminate pellets implanted in canine femora. Because of the reported presence of an osteoid seam which was believed to be caused by hydration of the ceramic (101), the authors of this paper conducted an investigation designed to evaluate bone growth into ceramic materials less likely to hydrate.

Pure aluminum oxide was chosen for this work because of its' reported biological inertness (38), high strength (53, 81), easy forming, and because facilities and technology were available for fabricating the necessary pore geometries.

Fabrication of Samples

The calcium aluminate pellets used in this study were fabricated according to the technique reported by Klawitter (55). To insure uniformity, all pellets were pressed from the same mixture of calcium carbonate and alumina, and fired at the same time.

The aluminum oxide pellets were made from Reynolds Company DB 152 low soda alumina with an average particle size of 1.6 microns. Using a small particle size enabled sintering of the alumina at a lower temperature than normally required (53). The sintering temperature used was 1485 degrees Centigrade.

Porosity was produced in the alumina using a foaming technique similar to that reported by Ryshkewitch (81) on the compressive strength of porous sintered alumina oxide and work done at Clemson University by Leonard (61).

Hydrogen peroxide[1], 6 percent, was used as a

---

1. Purepac Corporation, Elizabeth, New Jersey

chemical foaming agent, and polyvinyl alcohol solution consisting of .2 gram polyvinyl alcohol powder per 100 milliliters of distilled water, was used as a binder. Ryshkewitch noted that by varying the ratio of hydrogen peroxide to polyvinyl alcohol, the pore structure could thus be adjusted. By performing a series of trial and error preliminary foamings, a composition was chosen based on pore size and shape, percent porosity, and uniformity of the pore structure. Particular emphasis was placed on the pore size distribution because, as reported by Klawitter (55), to obtain mineralized bone ingrowth pores must have surface openings of at least 100 microns. It was found important to always use fresh hydrogen peroxide and polyvinyl alcohol solutions, for when they were allowed to set for a few days, they began to act inconsistently.

The following quantities, chosen to fill the required mold's volume, were hand mixed with a stainless stell stirring rod in a 100 milliliter polypropylene disposable beaker to form a uniform slurry; 100 grams aluminum oxide, 50 milliliters polyvinyl alcohol solution, and 50 milliliters hydrogen peroxide. This was poured into 1 1/2 x 2 1/2 x 5/8 inch open top aluminum molds and allowed to dry at room temperature for 24 hours. Large bubbles which appeared during stirring and pouring, could be eliminated by gently vibrating the filled mold. Aluminum molds were used because of the thermal conductivity values for aluminum.

After drying, many large bubbles were seen to have formed on

the bottom surface of some molds. It was found that polyethylene laid over the bottom prevented this.

The dried blocks were removed from the molds and fired on alumina setters in a silicon carbide electric resistance furance for twenty-four hours at 1485 degrees Centigrade. Samples were cooled to room temperature in the furnace.

During the foaming process there was a difference in drying rates in the horizontal and vertical directions causing a slight variation in the pore structure. Because of this and the presence of a highly dense outer layer on each block--approximately 2 millimeters--each block was ground equally in all directions towards the center when fabricating the samples for implantation and materials analyses so that each would be from the area with the greatest uniformity in pore structure.

Material Analysis

To characterize the mechanical and microstructural properties of the implant material, the following analyses were performed; apparent and bulk density, percent porosity and average pore size, compressive strength, and mercury porosimetry.

Density

Archimedes' method was used to determine the apparent and bulk

densities of 20 aluminum oxide samples, chosen randomly and cut on a high speed histological diamond saw[1] to specified dimensions. A hand micrometer was used to accurately measure each cut specimen to within ±.0001 inch from which the total volume of pores in the aluminum oxide was calculated (V_{total}). Each sample was then weighed in air to determine the weight of aluminum oxide (W_a), soaked in room temperature distilled water for 24 hours (after which no appreciable change in weight was detected) and again weighed while suspended in distilled water (W_{sus}). The apparent density of the aluminum oxide ($\rho_{apparent}$) was calculated:

$$\rho_{apparent} = \frac{\rho_w}{1 - (W_{sus} / W_a)} \qquad (1)$$

where (ρ_w) is the density of water (1 gm/cm^3).

The bulk density (ρ_{bulk}) was calculated:

$$\rho_{bulk} = \frac{\text{TOTAL WEIGHT}}{\text{TOTAL VOLUME}} = \frac{W_a}{V_{total}} \qquad (2)$$

A Mettler H6DIG GD balance was used for all weighings.

Percent Porosity and Pore Size

The percent porosity was determined by 2 methods: (a) using the known density, and (b) from a lineal analysis of 10 randomly chosen samples.

---

1. Brownwill Gillings Thin Sectioning Machine, Model 60, Brownwill Scientific, Rochester, New York

Using the already determined apparent density ($\rho_{apparent}$) and volume values for the previous 20 samples, the percent porosity was calculated:

$$\text{VOLUME OF OPEN PORES} = V_{total} - (W_a/\rho_{true}) \quad (3)$$

$$\text{PERCENT POROSITY} = 100 \times \text{VOLUME OF OPEN PORES} / V_{total} \quad (4)$$

A lineal analysis method (53) was also used to determine the percent porosity and the average linear pore size. To do this, the assumption had to be made that pores were uniform in size.

Ten typical samples taken as cross section of all foamings performed of the desired implant material, were placed in thick methyl methacrylate monomer[1] mounting media and allowed to polymerize. After complete hardening, the plastic block and sample was ground starting with 120 grit silicon carbide paper followed by 240, 320, 400, and 600 grit. Each block was ground so that a cross section of the vertical, longitudinal plane was shown.

A photomicrograph of each polished specimen was made on a Olympus Photomax vertical bright field illuminated microscope at 18.75X magnification using an attached 35 millimeter camera. A corresponding photomicrograph was made at the same magnification of a stage micrometer so that measurements from each photomicrograph could be accurately calibrated. A print was made from each negative resulting in a total magnification of 75X.

A set of 9 arbitrary lines were drawn on each photograph and

---

1. Matheson Coleman and Bell, Norwood, Ohio

the total number of pores that each line intersected (N_{pore}) were counted. The total length of the line crossing through each intersected pore was measured (L_{pore}) as well as the total length of all the lines drawn (L_{total}). From these values, the linear fraction (f_{pore}) of the pore diameters, which was equal to the percent porosity, and the average number of pores per unit length (N_a) was calculated for each print:

$$\text{PERCENT POROSITY} = f_{pore} = \frac{L_{pore}}{L_{total}} \tag{5}$$

$$N_a = \frac{N_{pore}}{L_{total}} \tag{6}$$

and according to Kingery (53):

$$\frac{f_{pore}}{2 N_a} = \frac{2}{3} r \qquad \text{or;} \quad D = 3/2 \frac{f_{pore}}{N_a} \tag{7}$$

where (r) is the average pore radius and (D) is the average linear pore diameter.

Mechanical Strength Testing

Load at fracture was determined for 10 randomly chosen aluminum oxide samples on a Baldwin-Tate hydraulic Energy Load Indicator according to the ASTM tentative method for testing "Compressive Strength of High-strength Ceramic Materials" (5). Each test specimen was cut into a 3/16 x 3/16 x 3/8 inch block on a precision histological diamond saw to insure dimensions and parallel faces. To reduce

shear stresses, a .0003 inch thick sheet of Teflon was placed at the interface of the specimen and the bearing plates. Tests were made on the 1,200 pound scale at a cross head speed of 5/32 inches per minute.

Compressive strength ($C_{fracture}$) was calculated from the following equation (5):

$$C_{fracture} = \frac{P_{fracture}}{A} \tag{8}$$

where ($P_{fracture}$) is the load in pounds required to cause failure of the specimen, and (A) is the cross sectional area in inches squared of the bearing surface of each specimen.

Mercury Porosimetry

The size of the pores and the bore of the interconnections between the pores in each implant are a very important factor in determining the type and depth of ingrowth which would be expected in both the surface and internal pores.

To obtain a characterization of the interconnection pore size, mercury porosimetry was performed on ten randomly chosen aluminum oxide samples. This would verify the size of the pores open to the surface that allowed mercury to enter upon application of external pressure. If the pores were very large, and the interconnections small, the size of the interconnecting orifice would be observed.

An Aminco 5-7212 mercury porosimetry analyzer with a range of from 0.012 to 100.0 microns pore size was used. The sample was weighed and then placed in a vacuum chamber. After the chamber was evacuated, mercury was introduced and the pressure increased to

2 pounds per square inch absolute so that it would fill the pycometer and stem. Then pressure was increased at set intervals and the volume of mercury intruded was measured.

A plot of pressure versus volume mercury intruded was made to determine the distribution of pore size interconnections.

Statistics

An understanding of the values obtained in the material analysis was dependent on a statistical interpretation. The arithmetic mean and medium were calculated for each material property investigated (60).

In Vivo Testing

Animal Selection and Maintenance

Female, 12 week old New Zealand white rabbits[1] were chosen for all implantation work because much of the early work by other authors on bone overgrowth and spur formations was done on rabbits, and because a preliminary surgical amputation indicated that rabbits

1. Cherokee Laboratory Supply, Atlanta, Georgia

would walk on their tibial stump. If this were so, the necessary forces required to maintain the normal mechanical stress patterns in the limb would be present, greatly enhancing the possibilities of obtaining bone ingrowth into the stump plugs. One other characteristic of rabbits is that the tibia and fibula unite in the middle third of the length of the leg to form a tibia-fibula junction.

It was the intention of the authors to minimize the variables by using animals of the same sex, age, and breed. Also, in the hope of having implants in during the maximum bone growth period, before the epiphyses close, the authors chose the animal age such that the longest implants would be sacrificed just prior to this age; in rabbit tibiae and fibulae this is approximately 5 to 7 1/2 months (35).

The rabbits were fed[1] and watered ad libitum and were maintained in 18 x 18 x 30 inch stainless steel cages. Each animal was kept for at least 2 weeks before surgery for quarantine purposes and to allow the animal enough time to adjust to the new environment, as advised by Bleicher (9).

Sample Preparation

Prior to surgery, the 2 types of implant shapes required for the *in vivo* analysis, cones and pellets, were hand ground on a silicon carbide matallurgical grinding wheel[2] to shapes determined

---

1. Purina Rabbit Chow, Ralston Purina Company, St. Louis, Missouri

2. Buehler Ltd., Evanston, Illinois

by presurgical radiographs and personal experience. The pellets, approximately 3 millimeters in diameter, were ground into a series of lengths ranging from 3 to 6 millimeters. Cone implants were shaped such that the largest diameter would be no larger than the major tibial diameter at the site of amputation and that the tip of the plug extend about 3 millimeters past the distal end of the stump.

Following the necessary shaping, the implants were prepared for surgery according to the following schedule:

(1) washed in a solution of distilled water and Ivory Flakes[1] in an ultrasonic cleaner[2] for 5 minutes to remove grease and other foreign particles present.

(2) rinsed in a polypropylene container under a hot water faucet, with vigorous agitation, for 2 minutes.

(3) washed in the ultrasonic cleaner with fresh distilled water for 2 minutes.

(4) rinsed in a sterile container under a distilled water faucet, with vigorous agitation, for another 2 minutes.

(5) autoclaved at 120 degrees Centigrade for 30 minutes using distilled water as a source of steam.

Animal Preparation

One day prior to surgery, each animal was taken off of feed. Anesthesia was administered preoperatively by 2 methods. The first

---

1. Ivory Flakes, Proctor and Gamble, Cincinnati, Ohio

2. Beckman Instrument Company, Fullerton, California

technique was to give an intravenous injection of sodium thiamylal[1] with atrophine sulfate[2] added, through an ear vein which was dilated by rubbing with an xylene saturated cottonball. Methoxyflurane[3] gas was administered, as needed, to maintain the proper surgical plane of anesthesia.

A second procedure was also utilized in which sodium pentobarbital[4] was administered intravenously as the primary anesthetic agent and either methoxyflurane gas or additional sodium pentobarbital used to maintain the surgical plane.

The surgical area on the animal was prepared by first removing the fur with electrical clippers with an Oyster number 40 blade. The skin was then scrubbed with 4 by 4 inch gauze sponges soaked in a providone iodine surgical scrub[5] followed by a rinse with 70 percent ethyl alcohol--3 consecutive times. Prior to surgical draping, a final providone iodine surgical spray[6] was applied.

Surgical Procedure

Three different procedures were performed in different combinations as determined by the implant group using aseptic techniques.

---

1. Surital, Parke-Davis, Detroit, Michigan

2. Atrophine Sulfate Injection, Schein Inc., Flushing, New York

3. Metophane, Pitman-Moore, Fort Washington, Pennsylvania

4. Pentobarbital Sodium Injection, Haver-Lockhart Laboratories, Shawnee, Kansas

5. Betadine Scrub, The Purdue Frederick Co., Yonkers, New York

6. Betadine Solution, The Purdue Frederick Co., Yonkers, New York

The amputations were performed through the middle 1/3 of the left leg just below the tibia-fibula junction. Approximately 2 centimeters below this point, a circumferential incision was made allowing the skin to be retracted to where the superficial fascia were exposed and incised. At this point the exposed muscle and muscle fasciae were severed, being careful to ligate all bleeders. The skin and muscle tissues were drawnback to the tibia-fibula junction to permit amputation. A high speed air drill[1] was used to transect the bone, smooth the edges, and to shape a socket for the cone implant, when applicable. The tissues were constantly flushed with saline solution for cooling purposes. When a cone implantation was made, digital pressure was used to seat the plug (see Figure 2a). The muscle flaps were lapped over the bone tip and sutured with 3-0 silk[2]. The skin was sutured with interrupted 4-0 monofilament nylon[3]. A topical antibiotic[4] was applied over the wound, followed by gauze and tape bandaging.

For the tibial pellets, an incision was made on the medial surface of the promixal 1/3 of the tibia. An orthopedic hand drill with a 3 millimeter diameter bit, was used to form a hole for the pellet. The specimen which was chosen to fit snuggly and approxi-

---

1. Hall Air Drill, Howmet Corporation, Medical Division, Rutherford, New Jersey

2. Measurol 3-0 Silk, Davis and Geck, Division of American Cyanamid Co., Danbury, Connecticutt

3. 4-0 Ethilon, Ethicon Inc., Somerville, New Jersey

4. Furacin, Eaton Laboratories, Norwich, New York

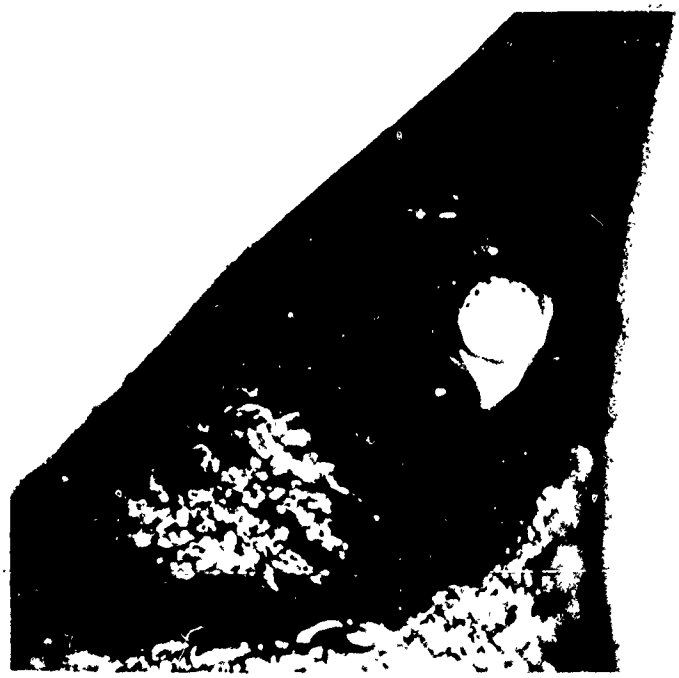

(a)

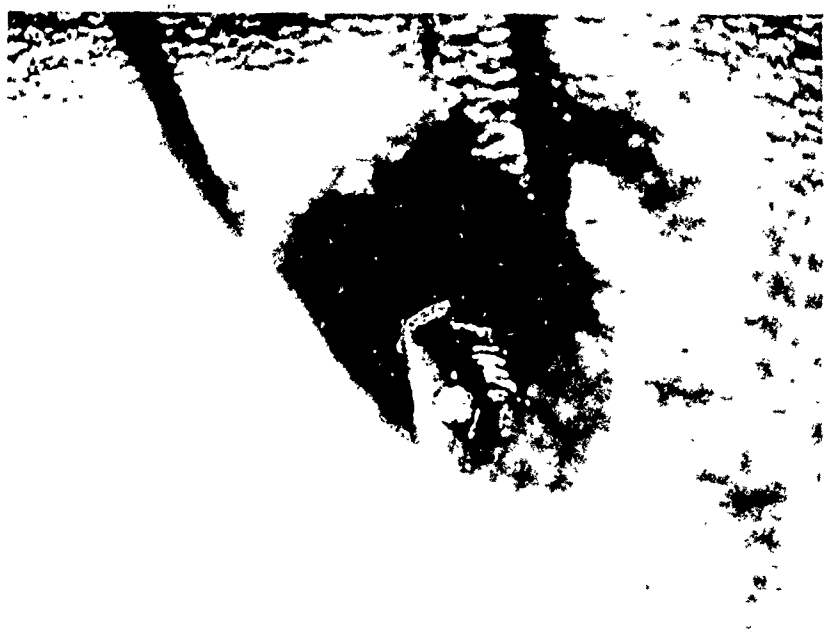

(b)

Figure 2. (a) Cone implant in place in the distal tip of the amputated tibia; (b) pellet implant in the lateral surface of the femur.

mately flush with the periosteal surface, was implanted under digital pressure. The incision was closed with 4-0 monofilament Nylon suture in a continuous pattern and a topical antibiotic applied.

The incision for the femoral pellets was made in the middle 1/3 of the femur. The previously mentioned technique was used to fit the pellet (see Figure 2b). 4-0 monofilament Nylon suture in a continuous pattern was made for closure followed by application of a topical antibiotic.

Following surgery, each animal received 1/2 cubic centimeter of penicillin and dihydrostreptomycin[1] antibiotic intramuscularly twice a day for 5 days.

In cases where the animal chewed the cutaneous sutures out, a plastic collar was placed around their neck, thus preventing access to the surgical wound.

Radiographs

Radiographs were made of each animal immediately post-operatively to check positioning of the implanted specimen. Two views were taken, medio-lateral and ventro-dorsal, to insure that the sample could be analyzed 3 dimensionally. Post-mortem radiographs were also made, following removal of all excess tissue, to examine the osteogenic response of the bone on a macroscopic level.

---

1. Penstrep, Merch Chemical Division, Rahway, New Jersey

Microradiography

In order to characterize the vascular network which develops in an amputation stump, a radiopaque liquid compound which would infiltrate arteries, veins, and capillaries was injected into selected animals. When the rabbit was to be sacrificed, sodium pentobarbital was administered through the ear vein to produce a surgical plane of anesthesia. The abdominal cavity was exposed so that both the abdominal aorta and the inferior vena cava could be cannulated with polyethylene tubing. The premixed liquid media was injected through a syringe attached to the cannule until a steady stream of the media drained from the cannulated vena cava--usually 80 milliliters was sufficient--after which both vessels were ligated and the carcass placed in a freezer. The limb could be radiographed either before or after fixation in the freezer.

The liquid microradiopaque media was mixed from the following: 48 milliliters MV - Diluent, 60 milliliters MV - 122 Yellow Microfil, and 3.2 milliliters MV Curing Agent[1]. The mixture had a viscosity of 160 Centipoise and a specific gravity of 1.30.

Histology

Fixation, Dehydration

After each animal was sacrificed, the excess tissue was removed from the implantation area, and the remaining specimen placed in 10 percent buffered neutral formalin fixative, (4.0 grams of sodium

---

1. Canton Bio-Medical Products Inc., Swarthmore, Pennsylvania

phosphate (dibasic, anhydrous), 100 milliliters of a 37-40 percent formaldehyde solution of formalin, and 900 milliliters of distilled water). Extra bone was cut away from the first animals sacrificed with an electric cast saw until it was discovered that this method cracked many of the fragile rabbit bones. Later, excess bone was cut away with a jewelers' saw. Because of the large specimen size, each block was left in fixative for at least 168 hours to insure thorough penetration.

Following fixation, the samples were placed in 70 percent ethyl alcohol to remove excess fixative which might interfere with staining properties and to begin dehydration. The samples were further dehydrated by 24 hour soaks in 80 percent, 95 percent and in absolute ethyl alcohol under a vacuum of approximately 300 millimeters of mercury.

Embedding

Two embedding mediae were tried, methyl methacrylate and Epon 812, to compare the overall application of each. Methyl methacrylate was first used because techniques had been perfected for producing high quality thin sections.

The first step following fixation and dehydration was to place the specimen directly in unpolymerized methyl methacrylate monomer with anhydrous benzoyl peroxide (1.0 gram/100 milliliters monomer) catalyst added, as described by Aga (103). This was possible because the alcohol is soluble in the monomer. The tissue block was left in thin monomer for 48 hours under approximately 300 millimeter vacuum. This process was repeated to insure that all of the alcohol

was removed. The sample was then placed in a 25 millimeter diameter, 100 milliliter test tube to which partially polymerized methyl methacrylate thick monomer was added. The thick monomer had been previously formed by heating thin monomer and catylyst at no higher than 80 degrees Centigrade until a syrupy consistency developed. The sample was allowed to completely polymerize at room temperature to prevent localized overheating which would damage tissue and leave bubbles within the matrix. Up to 720 hours were required for thorough hardening.

After removing the test tube and the unnecessary acrylic, the embedded specimens were fastened to 25 x 75 x 6.4 millimeter plexiglass blocks with acrylic cement.

Because it was very difficult to control the polymerization of the methyl methacrylate and very time consuming, a second technique using Epon 812 was tested. This embedding media could be easily mixed and stored and could be rapidly hardened at a low temperature--when needed (62).

After fixation and dehydration, the specimens were embedded using the following procedure:

(1) propylene oxide soak - 6 hours

(2) repeat step (1)

(3) soaked in a solution of 50 milliliters propylene oxide and 50 milliliters Epon 812 - 6 hours

(4) washed in 100 milliliters Epon 812 solution - 6 hours

(5) transferred with 100 milliliters of Epon 812 into a 250

milliliter polypropylene disposable beaker and placed under a 300 millimiter vacuum - 6 hours

(6) hardened in an electric heat furnace at 60 degrees Centigrade - overnight.

The Epon 812 solution used in steps (3), (4), and (5) was a solution of 50 volume percent of Epon 812, 50 volume percent methyl nadic anhydride hardener[1], and 1.5 volume percent of 2, 4, 6-Tri (dimethylaminomethyl) phenol (DMP-30)[2] catylyst. This solution can be stored in a refrigerator until needed.

Glass containers were satisfactory for steps (1) through (4), but it was necessary to use polypropylene tubes for step (5) to prevent cementing of the Epon to the container.

After hardening, the polypropylene tube was removed and the remaining block trimmed and mounted on a 25 x 75 x 6.4 millimeter Plexiglass block with epoxy cement[3].

Sectioning

After the samples were embedded, the mounts were firmly attached with 2 screws to the stage of the precision diamond saw so that thin sections could be cut (see Figure 3). Guaging the thickness of each cut is an art which, if perfected, will result in sections cut consistently at 75 microns and above at the operator's

---

1. National Aniline, Division of Allied Chemical and Dye Corporation, New York, New York

2. Rohm and Haas Company, Philadelphia, Pennsylvania

3. Buehler Ltd., Evanston, Illinois

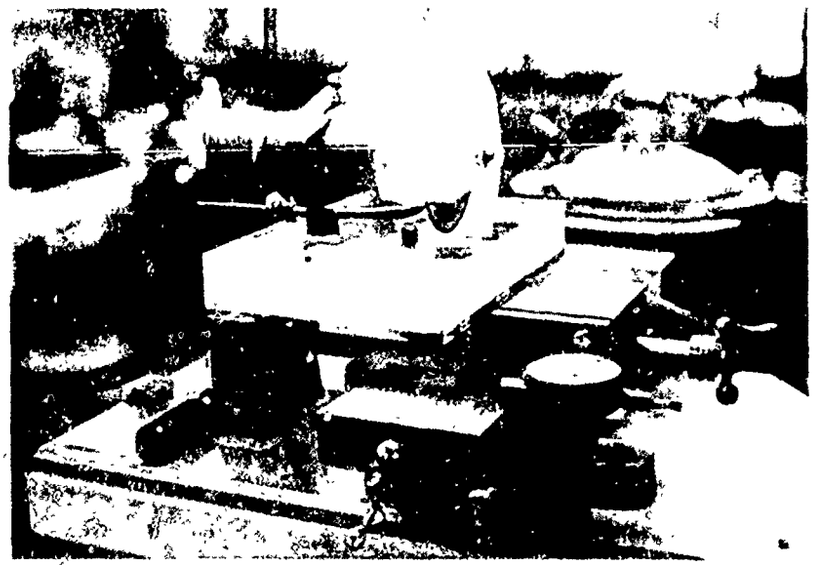

Figure 3. Precision diamond [illegible]

discretion. The blade speed was approximately 6500 revolutions per minute and the stage advance speed was about 9.5 millimeters per minute.

Pellet specimens were mounted so that sections were cut in 2 orientations; along the longitudinal and along the wide axes of the tibiae and femora. Cone implants were cut transversely to the stem of the implant. These orientations would permit maximum exposure of the ceramic-bone interface to microscopic and microradiographic examination (see Figure 4).

A technique similar to that reported by Klawitter (56) was used to produce hand ground sections. This was necessary because much of the microscopic anatomy was unidentifiable and often disallusioning because of multiplanar projections when examining sections greater than 100 microns thick. Fifty-five micron deep Well slides[1] were heated on an electric hot plate so that Canadian stick balsam[2] would just melt--not boil--forming a uniform liquid layer. The slide was placed on a flat surface and the section, 100 to 200 microns in thickness, set in the middle. Quickly, a piece of wax paper large enough to cover the entire slide, followed by a glass microscopic slide, were placed over the section and firm digital pressure applied while the balsam hardened. The microscopic slide and the wax paper were easily removed. The mounted section

---

1. Buehler Ltd., Evanston, Illinois

2. Ward's Natural Science Establishment, Rochester, New York

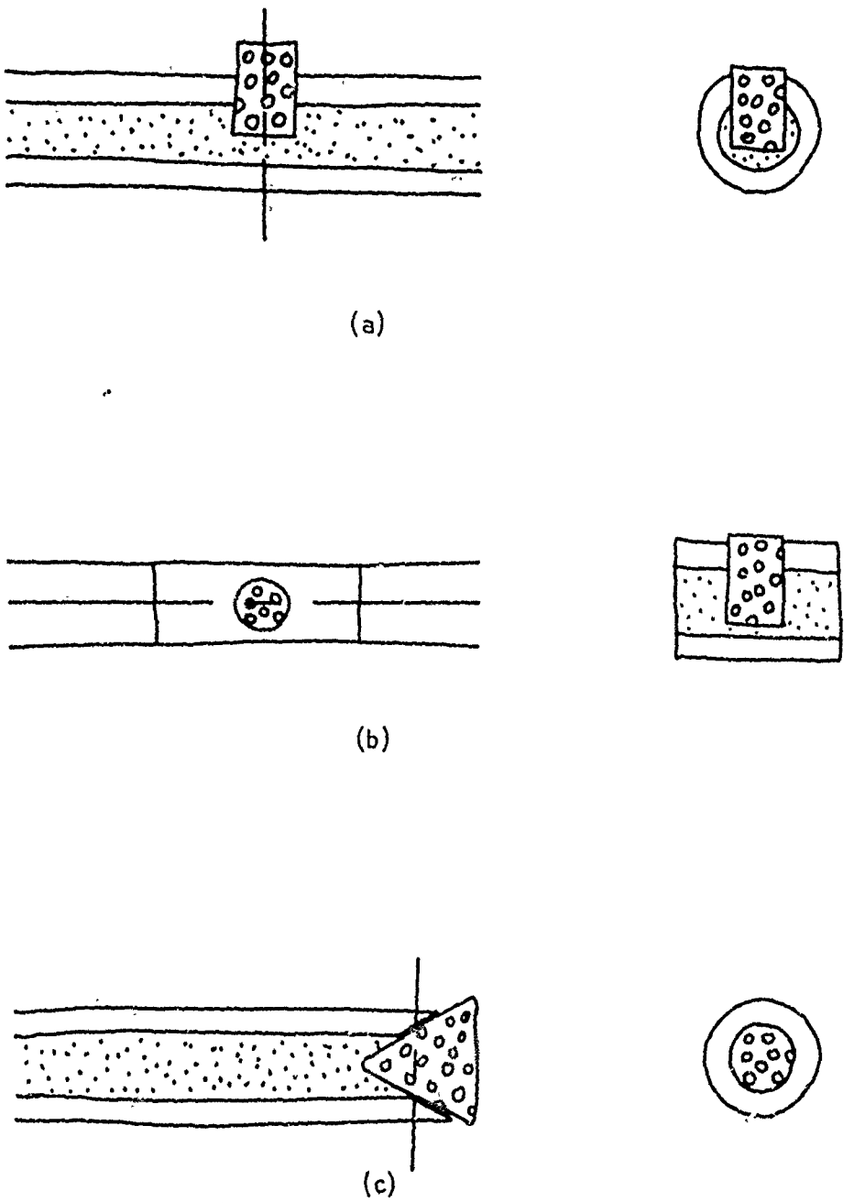

Figure 4. Orientations of thin sections: (a) cut along the longitudinal axis of a pellet shaped implant; (b) cut along the transverse axis of a pellet shaped implant; and (c) cut along the transverse axis of a cone shaped implant.

was then hand ground on a metallurgical polishing wheel to a thickness of from 25 to 75 microns with 320, 400, and 600 grit silicon carbide rotating discs under a continuous flow of water. Regular visual and microscopic checks were made to examine the thickness of the section and to inspect for tearing. A petrographic slide holder[1] was used to hold the slide during the grinding process. The slides were placed in absolute ethyl alcohol for 4 hours to dissolve the balsam. Xylene and toluene were not used because they also rapidly dissolved the mounting mediae. Sections were dried between 2 glass slides with a weight applied to prevent wrinkling.

Microradiography

A microradiographic technique was developed to characterize the areas of mineralized bone ingrowth because standard histological techniques often made it difficult to distinguish between osteoid and mineralize bone. By passing a fine beam of X-Rays through a histologic section directly in contact with an X-Ray sensitive emulsion, Jowsey (48) reported that the radiation absorption of the hydroxyapatite mineral phase of bone--calcified bone--was far greater then for a corresponding area of biological tissue of primarily protein constituents; osteoid, the lacunae of osteocytes, hemopoietic tissue, and muscle. Also discernible are osteons of low density where new bone is being formed. The ceramics are intrinsically radiopaque. This phenomena would provide a reliable technique for differentiating between mineralized bone and osteoid,

---

1. Buehler Ltd., Evanston, Illinois

and also provide a dependable contrast map of the areas and geometries of the calcified bone for each section microradiographed (54,74). Because this is a non-destructive testing technique, there is the added advantage that sections could also be stained for further histological comparison.

An apparatus designed by Klawitter (56) was used. The apparatus uses a source of X-Ray radiation[1] approximately 2 millimeters square, that is transmitted to a special light tight specimen-film holder (see Figure 5). The film and specimen are retained in direct contact by the application of a vacuum over the light tight black paper cover. A retaining ring is used to simplify handling.

Using Kodak type SO-343 high resolution spectroscopic film[2], the greatest contrast was obtained when the tube was operated at 20 milliamperes and 20 millivolts for an exposure time of sixty minutes. The specimen-film holder was placed 25 centimeters from the X-Ray source.

The films were developed[3] for 5 minutes, washed for 1/2 minute, and fixed for 5 minutes--all at 20 degrees Centigrade. The re-

---

1. General Electrix XRD-6 X-Ray Diffractometer, General Electric X-Ray Department, Milwaukee, Wisconsin

2. Kodak High Resolution Estar Thick Base Safety Film, Type SO-343, Eastman Kodak Company, Rochester, New York

3. Kodak D-19 Developer, Eastman Kodak Company, Rochester, New York

Figure 5. Specimen-film holder for microradiography.

sulting microradiograph was trimmed and mounted with a standard microscopic glass slide and cover slip using Permount[1] mounting media.

Staining

A staining technique was developed which would identify the different tissue components and cellular details of the cut and ground sections by their color reactions.

Many of the common biological stains are not able to penetrate either methyl methacrylate or Epon 812 embedding mediae consistently and rapidly enough to provide well detailed histological sections (86). The procedures that have been reported to be successful for staining these sections necessitated thicknesses of less than 2 microns (27, 43, 47).

A staining procedure was developed using Paragon-1301[2], a commercially available polychromatic stain, for 25 to 175 micron thick formalin fixed, methacrylate and Epon embedded sections.

Sections which were radiographed or not ground were mounted on Well slides using the technique previously described, and any balsam which might have passed over the surface of the section removed using a metallurgical grinding wheel with 600 grit silicon carbide paper. Obtaining analogous surfaces between the microradiographs and the histologic sections was still possible because

---

1. Fisher Scientific Company, Fair Lawn, New Jersey
2. Paragon-1301, C & C Company, Inc., Bronx, New York

great care was taken to insure that an insignificant amount of the section was ground away while removing the excess balsam. Sections which were ground and not radiographed required no modifications prior to staining.

The mounted sections were placed on an electric slide warmer at 50 degrees Centigrade and 2 drops of Paragon stain applied.

Methyl methacrylate sections were left until the stain had completely dried--with a glossy surface appearance--which took about 5 minutes. There were then flushed thoroughly with tap water and dried so that a light microscope examination could be made to insure proper staining. Excess stain was removed with ethyl alcohol, and further staining was accomplished by repeating the above steps for decreased time periods.

Epon embedded secitons were removed from the slide warmer after from 1 to 3 minutes, flushed under tap water, and dried. The procedure was repeated for additional staining.

Glass cover slips were affixed with Permount mounting media and excess media and bubbles removed with a xylene soaked cotton swab.

The observation of the staining reactions for the Paragon stained, methacrylate embedded sections indicated (10, 55, 71):

Nuclei - deep blue to gray

Nucleoli - dark blue

Cytoplasm - blue to gray

Erythrocytes - orange to red

Collagen fibers and elastica of blood vessels - red

Extracellular components of mineralized bone - unstained

Osteoid - pink

The Paragon, Epon embedded sections stained the following colors (86):

Nuclei - blue

Nucleoli and chromatin - dark blue

Cytoplasm - pink

Erythrocytes - orange to red

Collagen fibers - red

It was noted by the author that in most cases where Epon was used the marrow cavity and large porous areas within the cortical bone were not hardened completely, causing overstaining. It was not determined if the insoluble fats in these areas caused the problem or if soaking times in propylene oxide and Epon 812 solution were insufficient.

Slide Analysis

Because of the large number of sections to be anlayzed, it was necessary to organize a qualitative method of grading each slide on the most meaningful variables. Specific characteristics which could not be represented by this method were recorded for later reference.

Since, on the average, 6 sections could be cut either parallel or perpendicular to the stress lines of the bone from each pellet implant, the 3 middlemost sections were always analyzed to

insure uniformity in the grading method.

The variables were rated qualitatively by the authors using the following grading scales as a basis:

(a) Mineralized bone ingrowth into surface pore areas:

5 Excellent - all of the surface pore areas were completely infiltrated with mineralized bone

4 Very Good - greater than 3/4 of the surface pore areas were infiltrated with mineralized bone

3 Good - from 1/2 to 3/4 of the surface pore areas were infiltrated with mineralized bone

2 Fair - from 1/4 to 1/2 of the surface pore areas were infiltrated with mineralized bone

1 Poor - less than 1/4 of the surface pore areas were infiltrated with mineralized bone

(b) Mineralized bone ingrowth into internal pore areas:

5 Excellent - all internal pore areas were completely infiltrated with mineralized bone

4 Very Good - greater than 3/4 of the internal pore areas were infiltrated with mineralized bone

3 Good - from 1/2 to 3/4 of the internal pore areas were infiltrated with mineralized bone

2 Fair - from 1/4 to 1/2 of the pore area was infiltrated with mineralized bone

1 Poor - less than 1/4 of the internal pore area was infiltrated with mineralized bone

The areas graded for each implant was that directly between the surfaces of contact with the cortical bone.

(c) Condition of the periosteum; and (d) Condition of the endosteum:

5 Excellent - no abnormal changes present

4 Very Good - less than 1/4 of the surface showed signs of excessive porosity

3 Good - from 1/4 to 1/2 of the surface showed signs of excessive porosity

2 Fair - from 1/2 to 3/4 of the surface showed signs of excessive porosity

1 Poor - greater than 3/4 of the surface showed signs of excessive porosity

CHAPTER V

RESULTS

Material Properties

The average apparent ($\rho_{apparent}$) and bulk (ρ_{bulk}) densities for aluminum oxide, as determined by applying Archimedes principle, are 4.07 gm/cc and 1.57 gm/cc, respectively. The apparent density value compares favorably with the true density reported in The Handbook of Chemistry and Physics (95) which reports it to be 3.965 gm/cc relative to water at 25 degrees Centigrade.

The average percent porosity for aluminum oxide was determined using the calculated apparent density to be 62 percent; and using a lineal analysis to be 54 percent. Photomicrographs of the pore structures of the ground surface of each of the ten embedded aluminum oxide samples indicated that the pores were highly interconnected because of the complete impregnation of each pore with methyl methacrylate.

The average linear pore diameter was measured to be 390 microns. Listed in Table 1 is a comparison of some physical properties for porous aluminum oxide and calcium aluminate.

The compressive strengths varied widely for the ten specimens as shown in Table 2. Each specimen examined after failure had a wedge shaped appearance indicating that the bearing plates were satisfactorily parallel and that there was negligible shear between the contact surfaces. The apex and base of the wedge were in contact with the surfaces of the testing apparatus.

Table 1. Physical Properties of Porous Aluminum Oxide and Calcium Aluminate.

	Aluminum Oxide (Al_2O_3)	Calcium Aluminate ($CaAl_2O_4$)
Apparent Density		
Average (gm/cc)	4.07	3.04(2)
Median (gm/cc)	4.06	---
True Density	3.965(1)	---
Bulk Density		
Average (gm/cc)	1.57	1.58(2) 2.03(3)
Median (gm/cc)	1.57	---
Average Volume Fraction of Pores		
Known Density Method	.62	.48
Lineal Analysis Method	.54	---
Point Counting Method	---	.51
Solubility		
Cold Water	Insoluble(1)	Decomposes(1)
Acid, Alkali	Very Slightly Soluble(1)	---
Pore Diameter		
Average (Microns)	390	265(3)
Median (Microns)	380	---

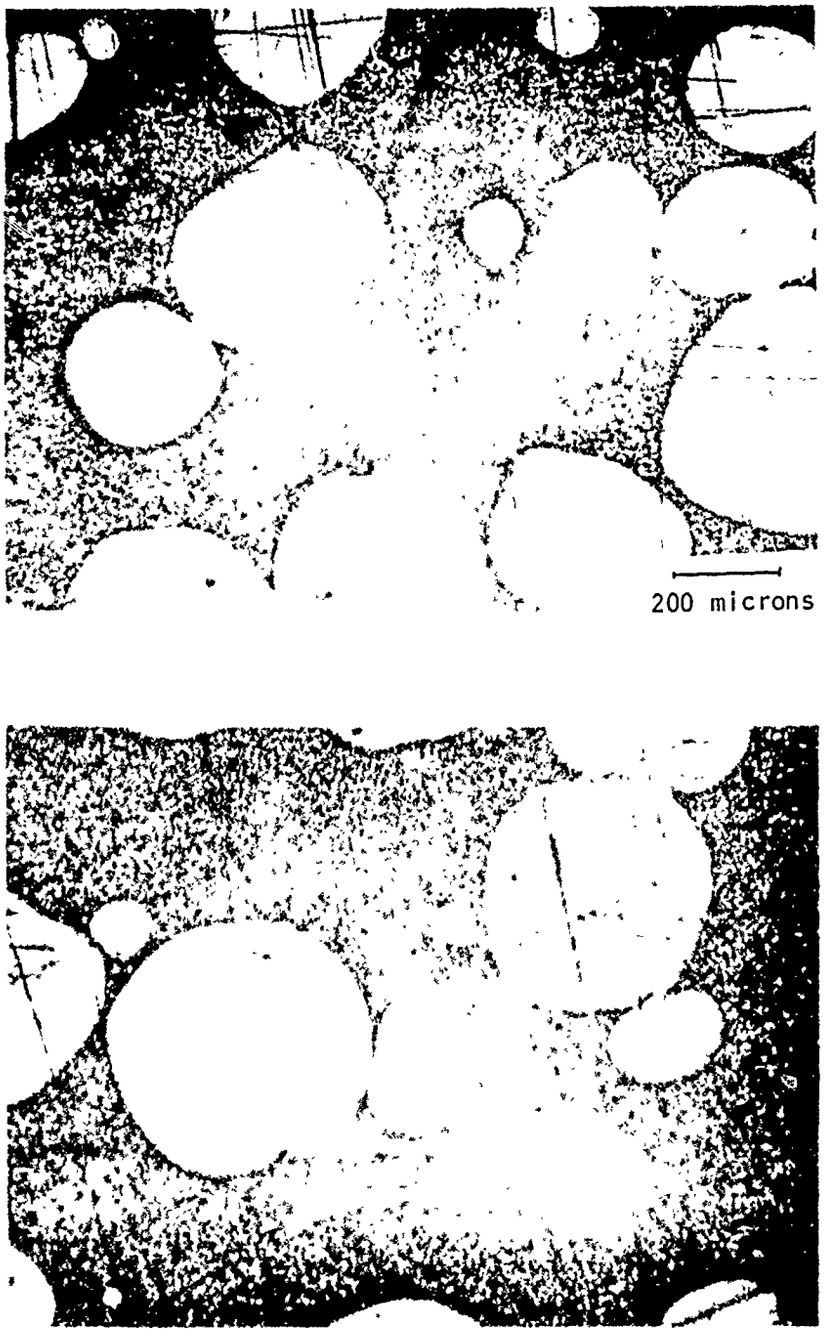

Figure 6. Photomicrographs of a transverse plane through two aluminum oxide specimens.

Figure 7. Photomicrographs of a transverse plane through two calcium aluminate specimens.

Table 2. Compressive Strength of Porous Aluminum Oxide (psi).

Average	3440
Median	3120
Maximum	4540
Minimum	2590

The distribution of the pore interconnection is shown in Table 3. The data is based on the microstructure analysis of ten randomly selected specimens.

In Vivo Analysis

A gross examination of the specimen and surrounding tissues prior to fixation in buffered formaline revealed no sign of inflammation or abnormal tissue reaction around any of the aluminum oxide or calcium aluminate implants or at the site of amputation. The surgical incisions were all well healed with no evidence of infection or non-union of the tissues.

Cone Implant Group

Left Tibia - Al_2O_3

The post-mortem radiographs of the 4 and 8 week implants indicated an interspace approximately 200 microns wide between the implant stem and the endosteal surface of the distal end of the tibia. The space was interrupted at a few points where spicules of mineralized bone appeared to connect the implant to the wall of the cortical bone (see Figure 8).

Table 3. Histogram of the Distribution of Pore Interconnections

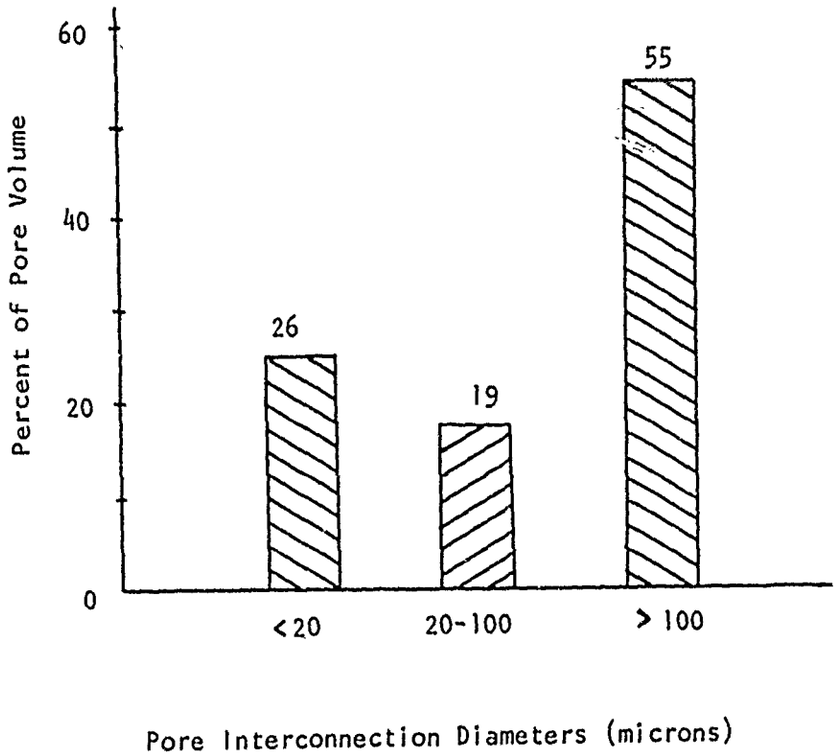

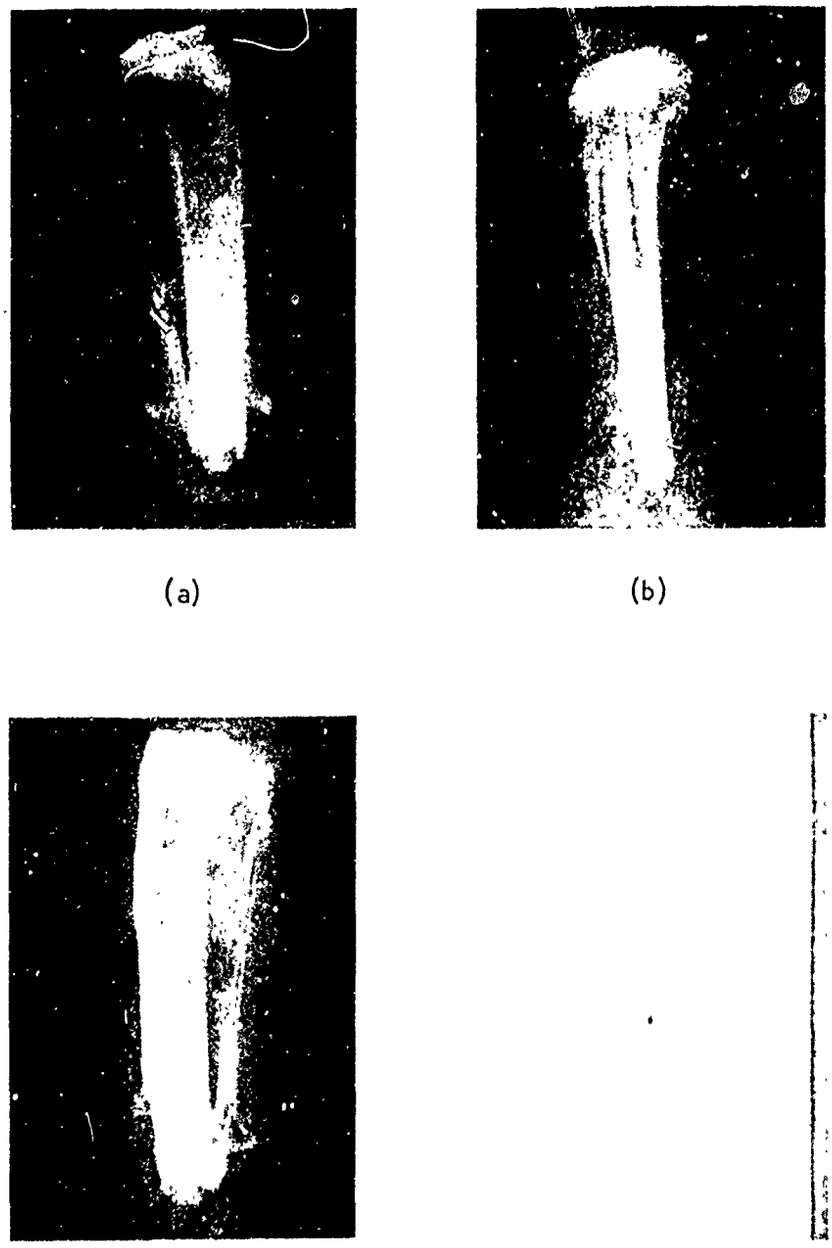

Figure 8. Radiographs of aluminum oxide cone implants in the left tibia of the CONE IMPLANT GROUP: Four week (a) anterior-posterior, (b) medio-lateral; Eight week (c) anterior-posterior, (d) medio-lateral.

In all cases, 2 bone spurs were present starting roughly 3 millimeters above the tip of the bone stump. The overgrowths, originating from the medial surface of the tibia and the lateral surface of the fibula, extended axially from the periosteal surface and then curled slightly so that its tip was directed towards the stump's neb. There were no signs of axial bone overgrowth. The authors did not determine whether or not the epiphyses were still open.

A histological analysis used in conjunction with a micro-radiographical analysis of the 4 week implants demonstrated very limited bone ingrowth into surface pores and far less into the internal pores.

The arrangement of the bone which did project into the surface pores was that similar to tree branches originating from the endosteal surface (see Figure 9). The remaining pores were saturated richly with vascularized connective tissue as was most of the space between the implant and the interior surface of the tibial bone (see Figure 10a).

In most cases, the overall bone geometry was porous with a great deal of abnormal bone overgrowth directed vertically from the tibial shaft. The large number of porous areas which were present within the overgrowths were well lined with osteoblasts, typical of intramembraneous ossification, although there were no signs of organized Haversian systems. In some instances, a distinct zone of endochondral ossification, characterized by cartilage cells,

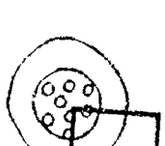

(a)

(b)

(c)

...implant in
...the lo-
...na (c)
...ferralized
...ter 4

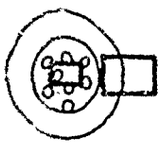

(a)

(b)

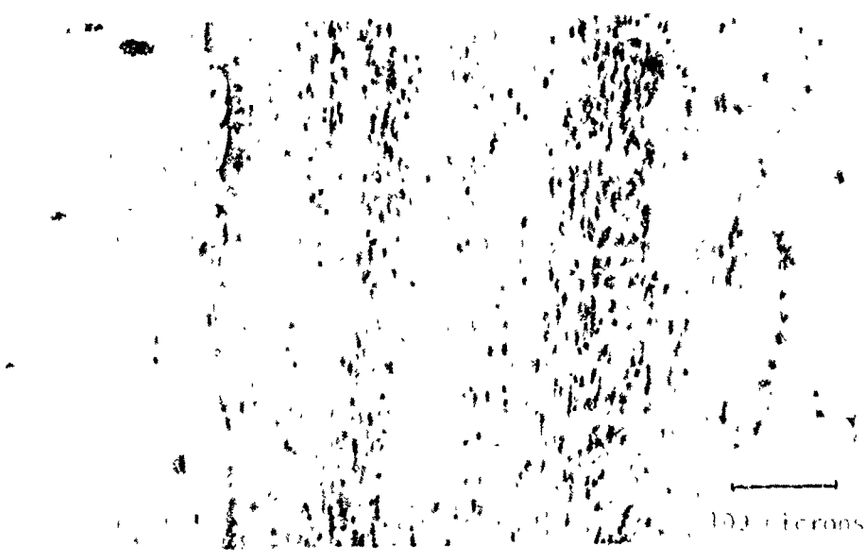

(c)

Figure 10. (a) Sketch of a transverse section from a cone implant [illegible] outlining the [illegible] through charring an internal [illegible] pellet saturated with loose [illegible] (b) a photomicrograph of [illegible] tissue surrounding [illegible]

was present around the outer spicules of bone comprising the overgrowth (see Figure 11). Where overgrowths were not present along the periphery of the tibia, the periosteum was very jagged and osteoclasts were visible. The corresponding endosteum appeared normal, but few osteoblasts were readily discernible. The porous areas within the mineralized bone which was bound by these surfaces were well lined with osteoblasts (see Figure 12).

Exterior to the outer perimeter of the tibia was dense collagenous scar tissue with a few traces of scattered muscle fibers which were always located near the overgrowths but not incorporated into its surface.

The segment of the cone shaped implant which protruded beyond the distal end of the tibia was well suffused with fibrous connective tissue as were the surface pores. The internal pores contained loose connective tissue. Dense collagenous scar tissue filled the area between the fibrous covering and the subcutaneous tissues (see Figure 10B).

The only distinguishable difference noted from the 8 week implants was that they showed more mineralized bone ingrowth although it was still very incomplete and of limited osteoblastic activity. The balance of the pore areas were filled with loose connective tissue (see Figure 13).

Cone Implant Group

Left Femur - Al_2O_3

Radiographs taken post-mortem of the 4 week implants demon-

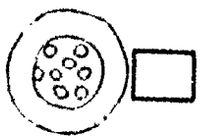

(a)

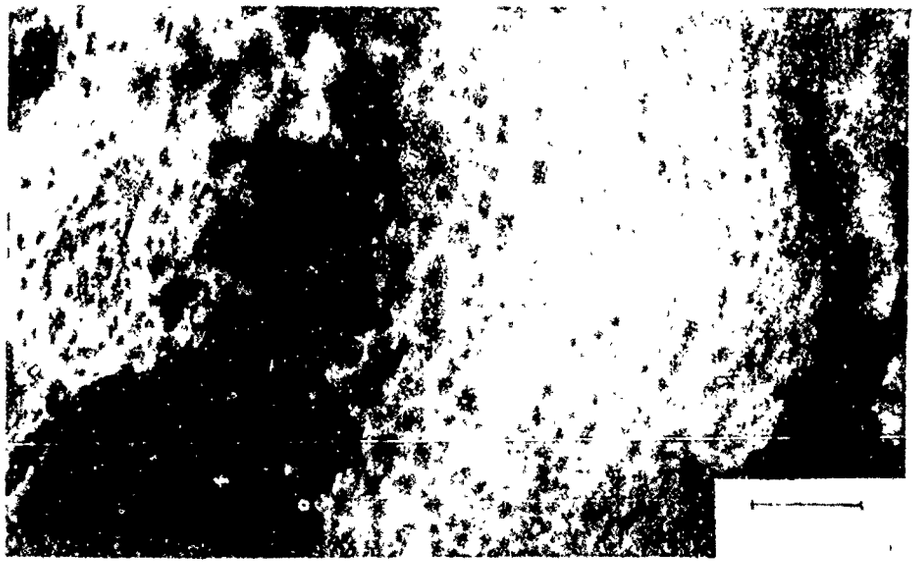

(b)

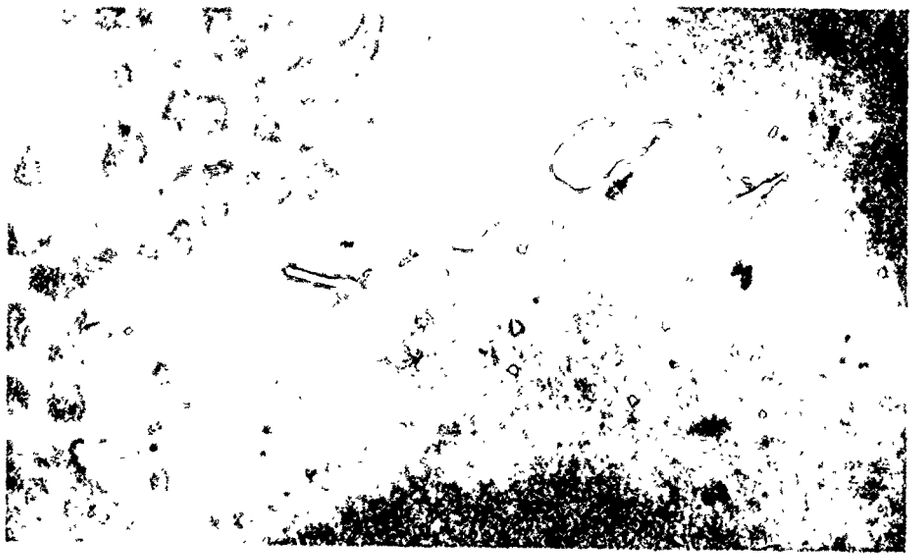

(c)

[illegible] one implant
[illegible] utilizing the
[illegible] ounding
[illegible] fection-

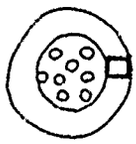

(a)

(b)

(c)

[illegible] (a) Sketch of a transverse section from a cone implant in the tibia from the CONF [illegible] 10% outlining the location of a; (b) photomicrograph, and corresponding (c) [illegible] of the cortical bone at the distal end of the tibia after [illegible].

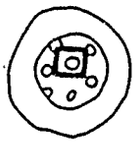

(a)

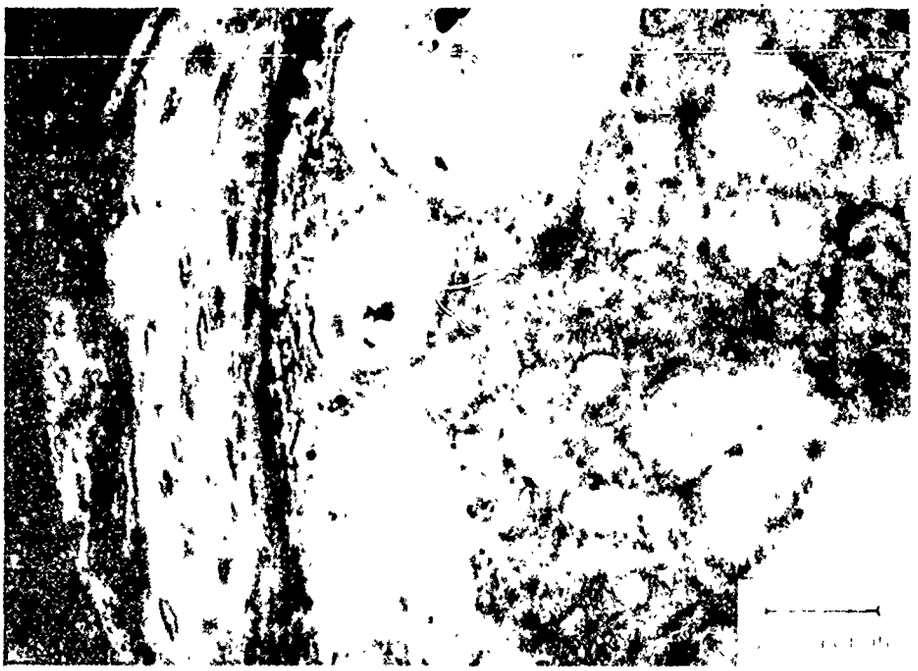

(b)

Figure 13. (a) Sketch of a transverse section from a cone implant in the tibia from the CONE IMPLANT GROUP outlining the location of a; (b) photomicrograph of an internal pore from an aluminum oxide pellet containing mineralized bone and loose connective tissue after 8 weeks.

strated areas immediately adjacent to the specimens which were less radiopaque than normal mineralized bone which would indicate that there was an interface between the implant and the cortical bone which was not completely calcified in some areas. There was also a slight thickening of the bone, similar to a callus formation, at the implantation site. The rest of the femur appeared radiographically uneffected (see Figure 14). The pellets implanted for 8 weeks were better incorporated into the normal architecture of the bone with little change in the radiopaquity around and immediately adjacent to the implant.

The histological and microradiographic analyses of the 4 week specimens supported the radiographic results. Surface pores were partially infiltrated with calcified bone with no sign of separation where bone was adjacent to Al_2O_3 (see Figures 15 and 16). There was, however, active osteoblastic activity on most bone surfaces at the interface.

The inner pores were permeated with hemopoietic tissue and very limited mineralized bone. The porous areas of the pellet which extended into the bone marrow also contained spicules of mineralized bone (see Figure 17b).

The exposed surface of the pellet was encapsulated with a very thin layer of fibrous connective tissue over which normal muscle tissue had immigrated (see Figure 17c). Inner pores adjacent to this site were also saturated with connective tissue.

The overall structure of the bone appeared completely normal except for limited porosity around the implant. There was no

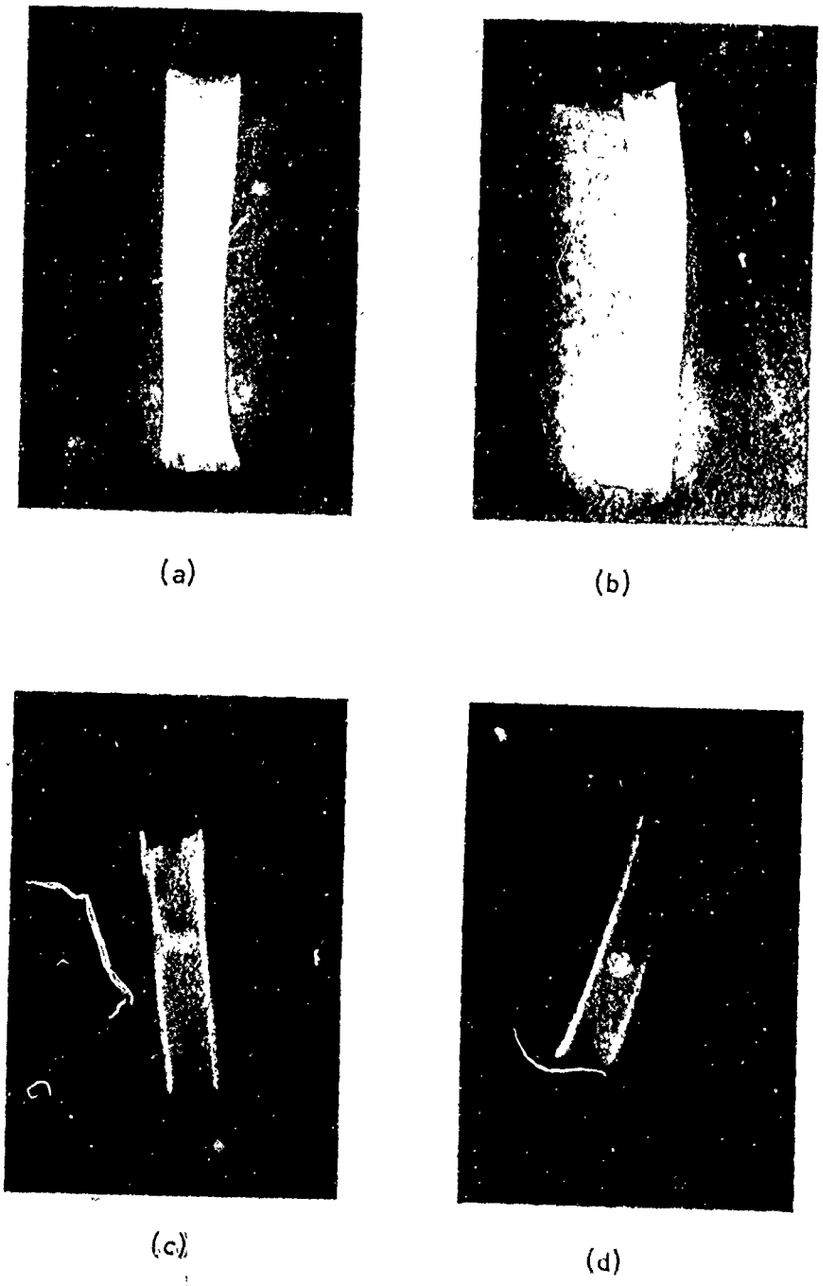

Figure 14. Radiographs of aluminum oxide pellet implants in the left femur of the CONE IMPLANT GROUP: Four week (a) anterior-posterior, (b) medio-lateral. Eight week (c) anterior-posterior, (d) medio-lateral.

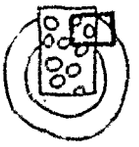

(a)

(b)

(c)

Figure 15. (a) Sketch of a cross section of a femur from the CONE IMPLANT GROUP outlining the location of (b) photomicrograph, and corresponding (c) microradiograph [illegible] partial mineralized bone matrix [illegible] fillet after 4 weeks.

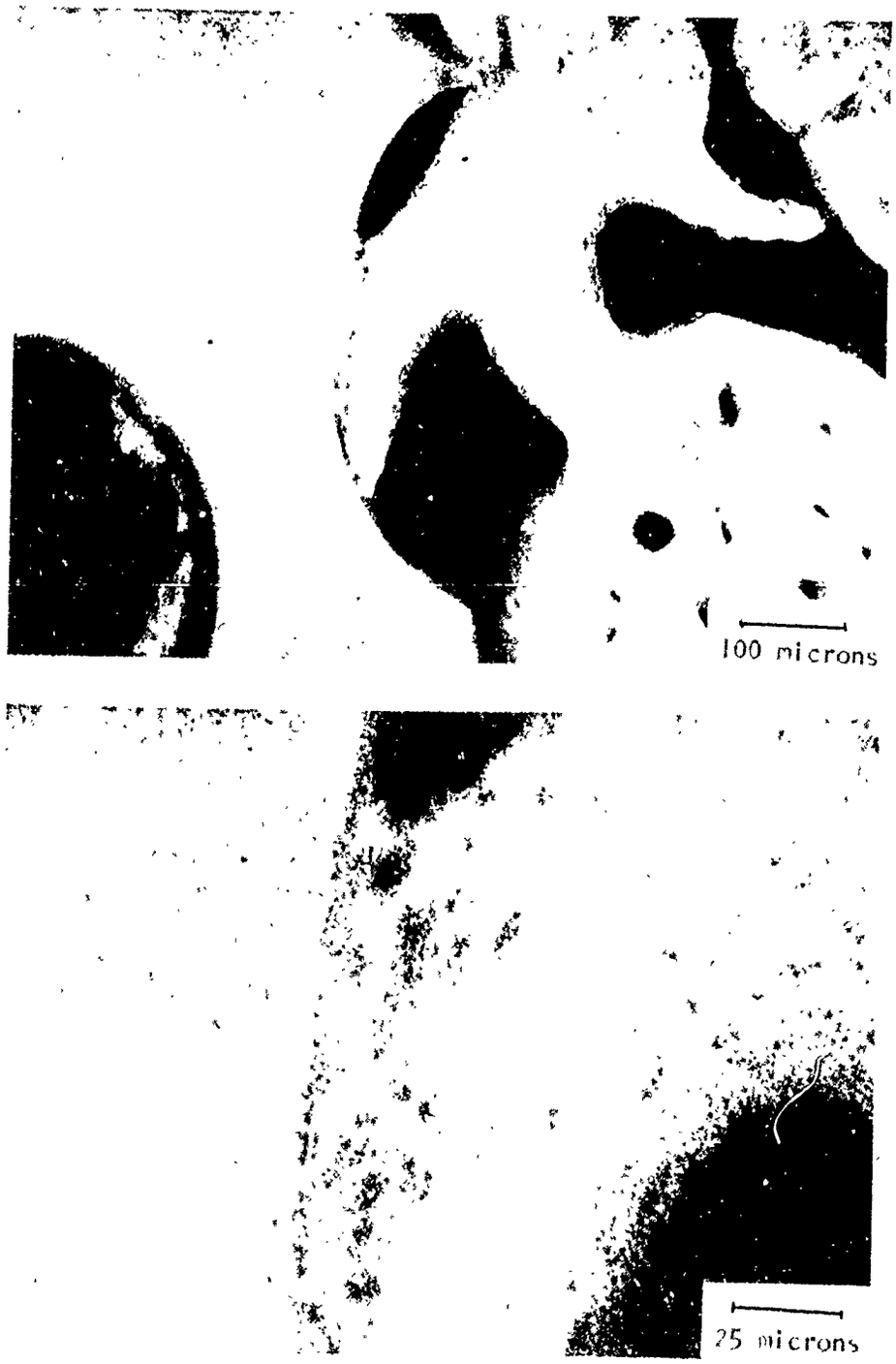

Figure 15. Area outlined in figure 15 at higher magnifications demonstrating the loss of amorphous phase.

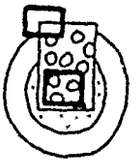

(a)

(b)

(c)

Figure 17. (a) Sketch of a cross section of a femur from the CONE IMPLANT GROUP outlining the location of a, (b) photomicrograph of spicules of mineralized tissue in an aluminum oxide pore within the bone [illegible] 4 weeks, and (c) photomicrograph of the [illegible] of the exposed tip of an aluminum oxide [illegible] implant after 4 weeks.

noticeable difference in the degree or type of ingrowth into the sections cut perpendicularly to the normal femoral stress lines and those sections cut parallel to the stress lines (see Figure 18).

The 8 week pellet implants showed very good calcified bone ingrowth into the exterior pores, extensive osteoblastic activity at the implant interface, and the presence of fine tunnel-like network of mineralized bone throughout most of the inner pores of the entire pellet (see Figures 19 and 20). There was no separation between bone and ceramic where they were abreast.

There was little or no change in the architecture of the femur outside the immediate radius of the implant. The corresponding periosteum, endosteum, and bone marrow appeared normal.

Pellet Implant Group

Left Tibia - Al_2O_3

Post-mortem radiographs indicated that there were 2 bone spurs present protruding up to 8 millimeters from the periosteal surface of the distal end of the tibia and fibula on most implants in this group. The overgrowths were on the average of 4 millimeters distal from the site of amputation on the medial surface of the tibia and the lateral surface of the fibula (see Figure 21). At the distal end of the tibia there was no recognizable evidence of axial bone overgrowth.

There was a slightly lighter area on each radiograph between the pellet and the mineralized bone of the cortex.

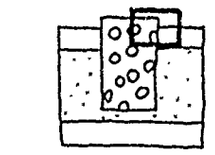

(a)

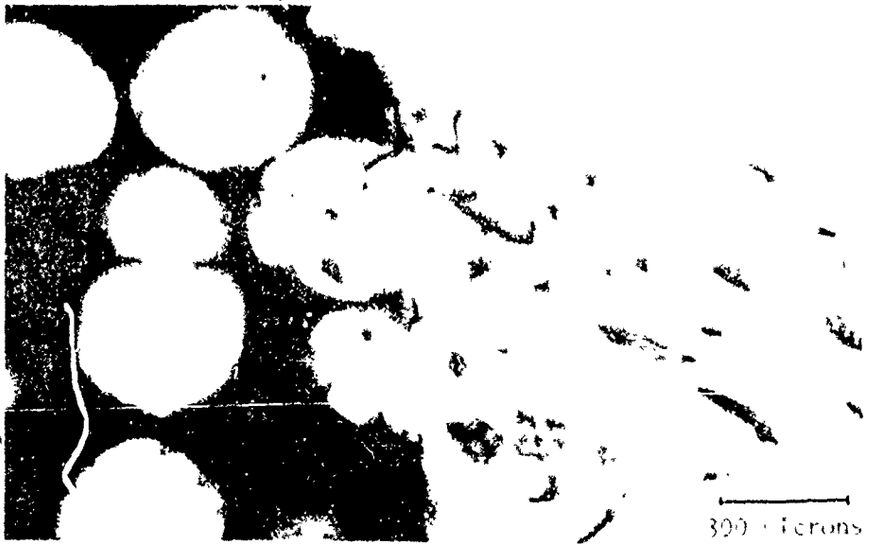

(b)

(c)

Figure 18. (a) Sketch of a longitudinal section of a femur from the CONE IMPLANT GROUP outlining the location of a; (b) photomicrograph, and corresponding (c) microradiograph demonstrating partial mineralized bone ingrowth into the [illegible] after 4 weeks.

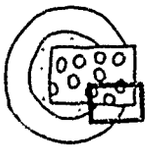

(a)

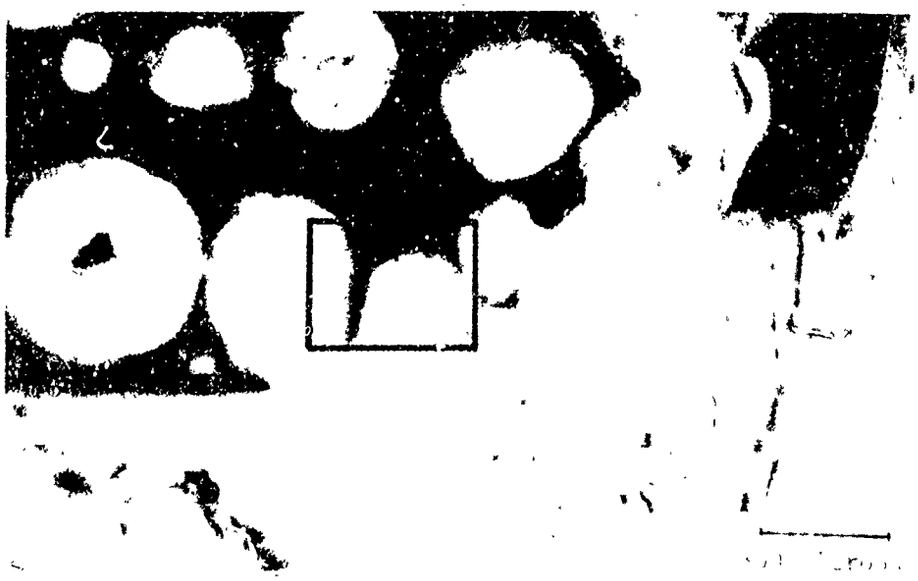

(b)

(c)

Figure [illegible]. (a) [illegible] (b) [illegible] the CONE IMPLANT [illegible] (c) [illegible] photo-micrograph [illegible] scanning [illegible] microscope [illegible] [illegible] into [illegible]

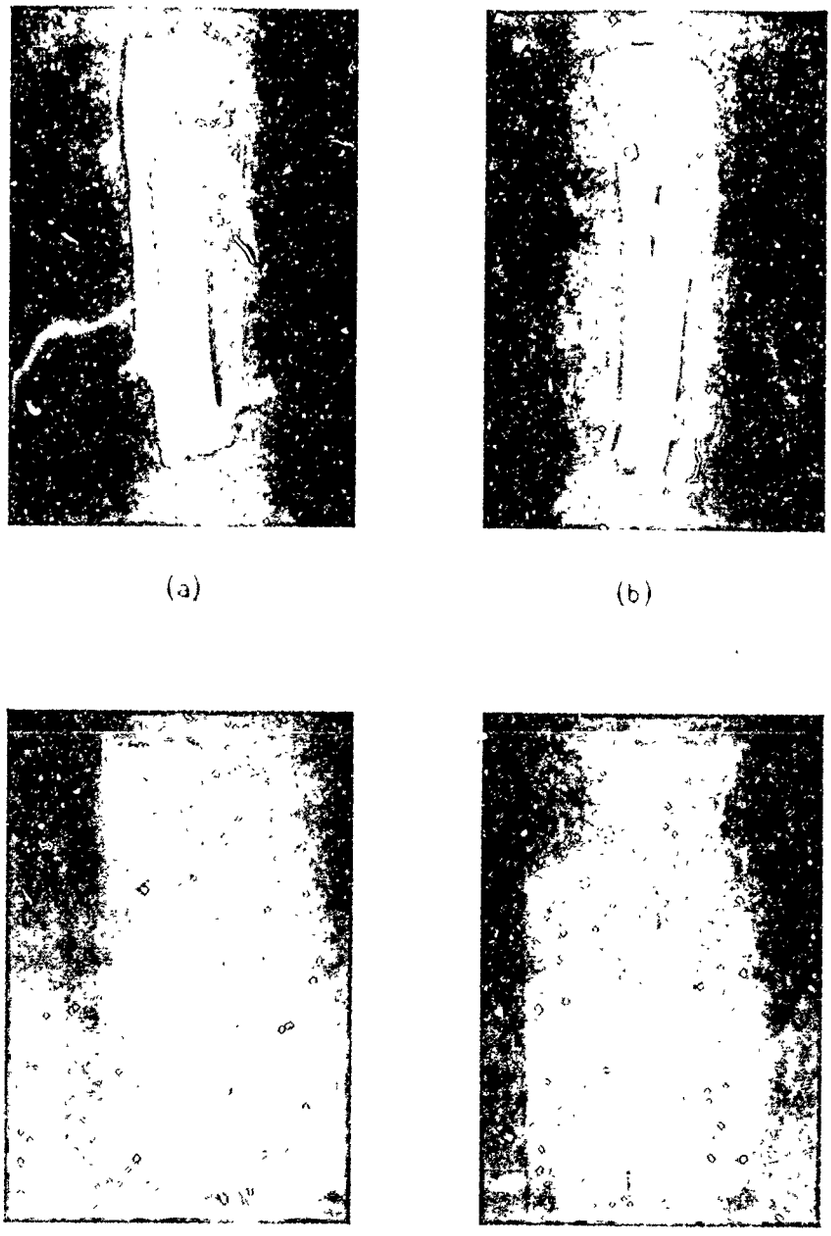

Figure 21. Radiograph of aluminum oxide pellet [illegible] of the PELLET [illegible] (a) [illegible] exterior-exterior, (b) [illegible] exterior-exterior, (c) [illegible] exterior-exterior, (d) [illegible]

The 8 week implants had similar spurs but there was no seam of uncalcified tissue present between the sample and the bone.

The histological and microradiographic sections showed that the distal tip of the tibia was completely infiltrated with spicules of mineralized bone, rich with osteoblastic activity (see Figure 22). The corresponding cortical bone of the tibial shaft was also porous. The periosteum had a "cookie-cutter edge" appearance with many osteoclasts visible.

At the site of the pellet implantation, from 30 to 70 millimeters above the site of the amputation, the endosteal surface appeared normal; but again the periosteum was very jagged, characterizing osteoclastic activity In many places, the corresponding cortical bone was also very porous. The bone ingrowth into the surface pores of the pellet was scattered and very porous, but these areas were lined with osteoblasts (see Figure 23). Sections made parallel to the longitudinal axis of the femur showed that the porous areas ran parallel to the Haversian systems of the cortical bone. The internal pores were suffused with hemopoietic tissue and a very limited number of mineralized bone spicules.

The tip of the pellet exposed at the periosteal surface was impregnated with fibrous connective tissue over which was normal skeletal muscle tissue.

The only difference visible in the 8 week implant sections was that there was a great deal more mineralized bone ingrowth into the surface and internal pores (see Figure 24).

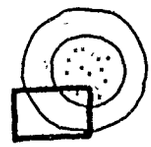

(a)

(b)

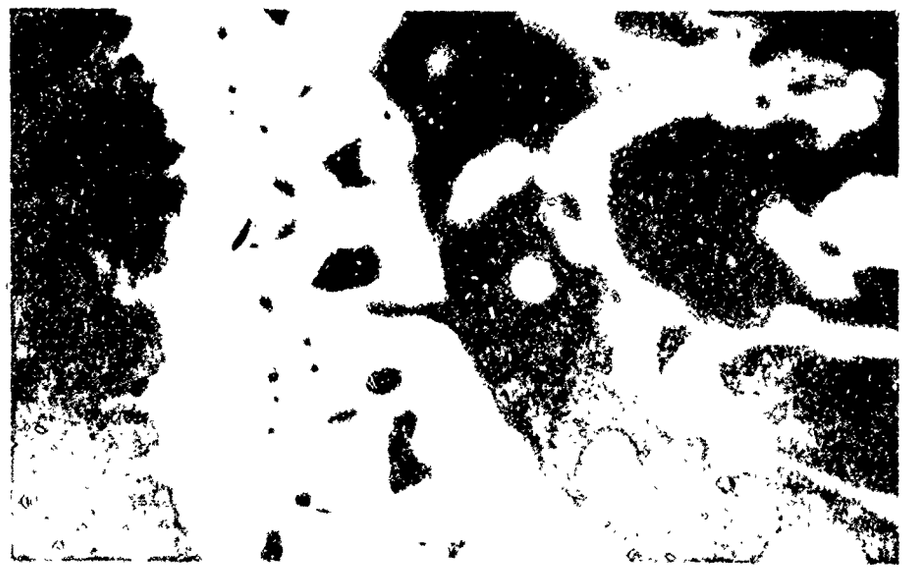

(c)

Figure 12. (a) Sketch of a cross section of a tibia from the PELLET IMPLANT GROUP outlining the location of a; (b) photomicrograph, and corresponding (c) microradiograph demonstrating infiltration of the distal tip with mineralized bone after 4 weeks.

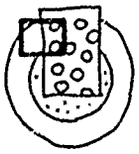

(a)

(b)

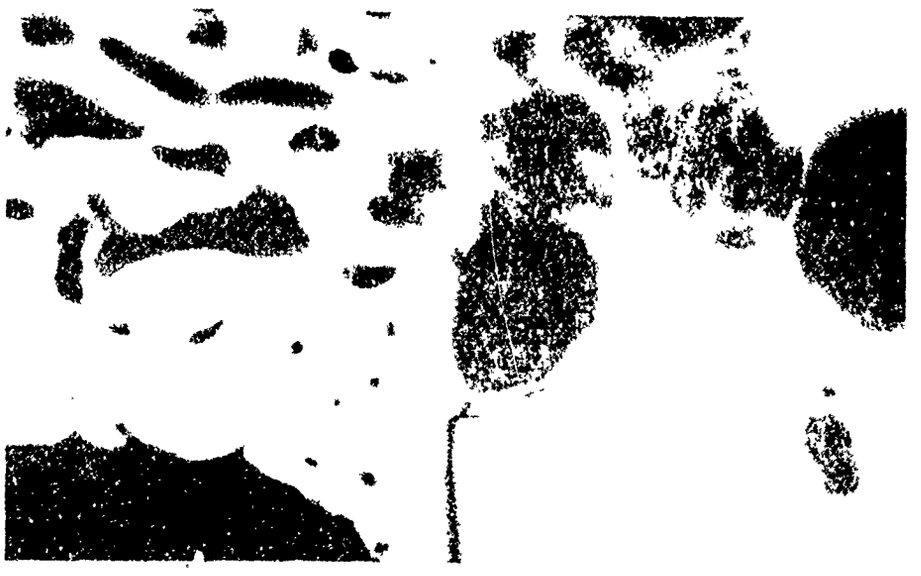

(c)

Figure 23. (a) Sketch of a cross section of a disk from the PELLET IMPLANT GROUP outlining the location of it; (b) photomicrograph, and corresponding autoradiograph demonstrating scattered fission fragment tracks emerging into the aluminum oxide pellet at the

Pellet Implant Group

Left Femur - Al_2O_3

The post-mortem radiographs revealed little difference between the femur pellets analyzed in the Cone Implant Group for the 4 and 8 week implant periods. In two cases, however, 8 week pellets were implanted below the periosteal surface causing the bone to remodel partially over and partially through the structure of the implant (see Figure 25).

There was a corresponding similarity of the histological and microradiographical sections. There was a great deal of ingrowth of mineralized bone in the surface pores of both the 4 and 8 implants (see Figures 26 and 27). The inner pores were partially lined with calcified bone which was well overlayed with osteoblasts and osteogenous and hematogenous bone marrow.

The cortical bone of the femur appeared completely normal in all cases.

Bilateral Implant Group

Right Tibia - Al_2O_3

The radiographs of the post-mortem 4 and 8 week aluminum oxide implants in the right tibiae under a normal stress condition, no amputation, indicated no abnormal bone changes outside the radius of the implant except in one case where a callus was present on the medial surface of the tibia protruding approximately 4.5 millimeters. There was no discernible interspace between the implant

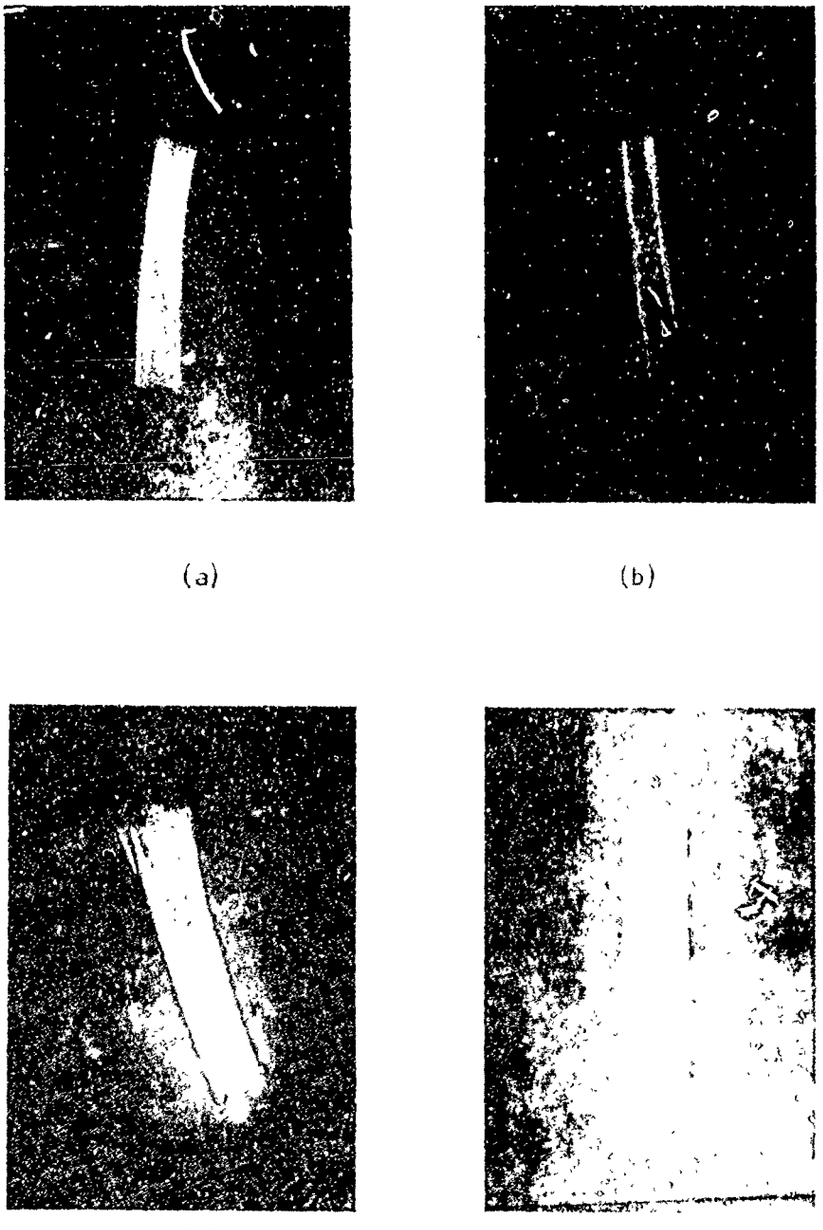

Figure 25. Radiographs of aluminum oxide pellet implants in the left femur of the PELLET IMPLANT GROUP: four weeks (a) mediolateral, (b) anterior-posterior. Eight weeks (c) mediolateral, (d) anterior-posterior.

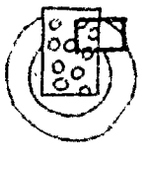

(a)

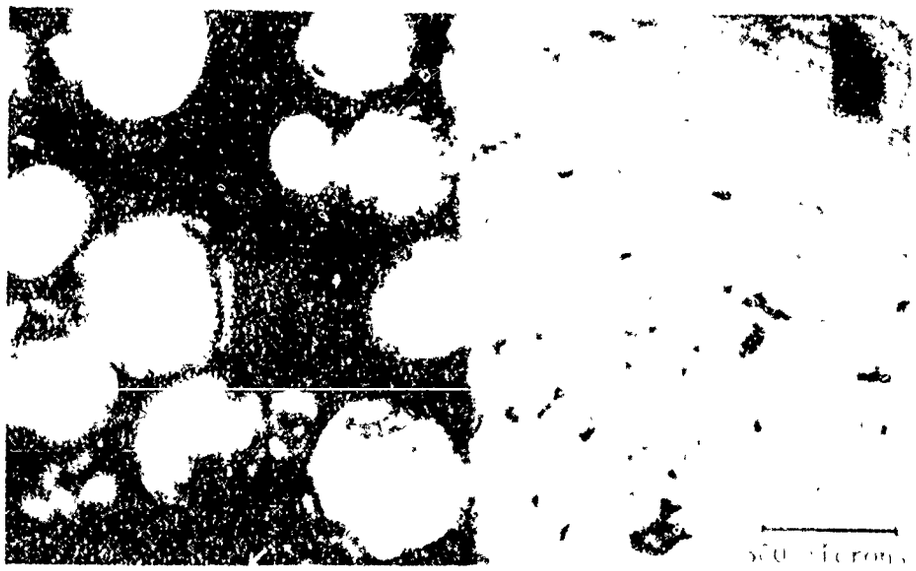

(b)

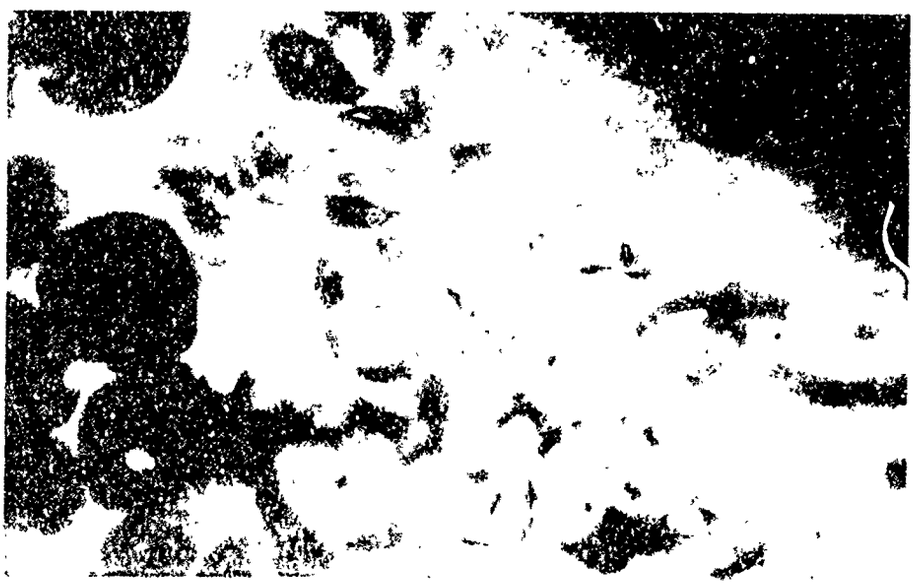

(c)

Figure 26. (a) Sketch of a cross section of a femur from the PELLET IMPL [illegible] with the location outlined of (b) photo-[illegible] and corresponding (c) [illegible] graph demon-[illegible] and mineralized bone [illegible] to the [illegible] after 4 week

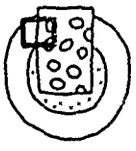

(a)

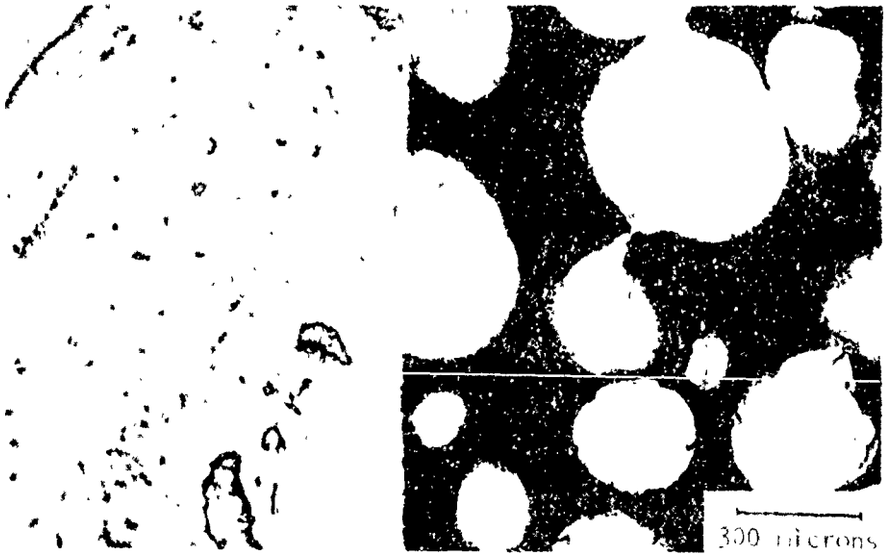

(b)

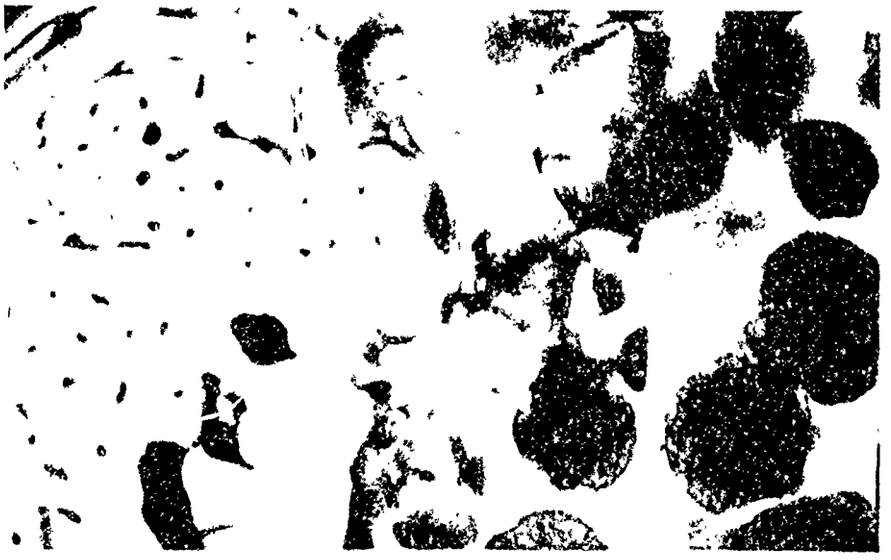

(c)

Figure 27. (a) Sketch of a cross section of a femur from the PELLET IMPLANT GROUP with the outlined location of a; (b) photomicrograph, and corresponding (c) microradiograph demonstrating very good mineral[illegible] an aluminum oxide pellet [illegible]

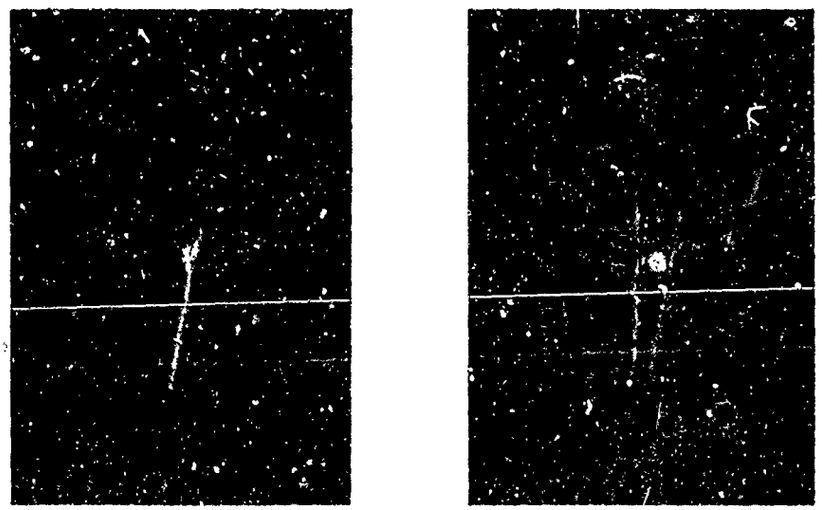

(a) (b)

Figure 28. [illegible] of an aluminum [illegible] in the right femur of the BEAGLE, [illegible] four weeks; (a) radio-lateral, (b) anterior-[illegible]

and the mineralized bone. On the average the pellets were located roughly 50 millimeters above the tibia-fibula junction (see Figure 28).

The histological and microradiographical examination of the 4 week specimens showed good surface ingrowth with an extensive network of interconnected, calcified bone spicules on the surfaces of most internal pores. Stained sections revealed a thorough permeation of the remaining pore areas with osteogeneous and hemotogeneous bone marrow (see Figure 29).

The 8 week implants showed even greater mineralized bone ingrowth into the surface and internal pores (see Figure 30).

The cortical bone of the tibiae and fibulae appeared unchanged.

Bilateral Implant Group

Right Femur - Al_2O_3

Radiographs of the 4 and 8 week samples taken post-mortem showed no change in the overall structure of the femur except for cases were the tip of the pellet implant protruded past the periosteal surface, where a bony callus developed over the protrusion similar to that found in fracture healing (see Figure 31).

The histological and microradiographic analysis of the 4 week implants confirmed the radiographical results of very good mineralized bone ingrowth into the surface pores and the lack of any seam between the ceramic and bone (see Figures 32 and 33).

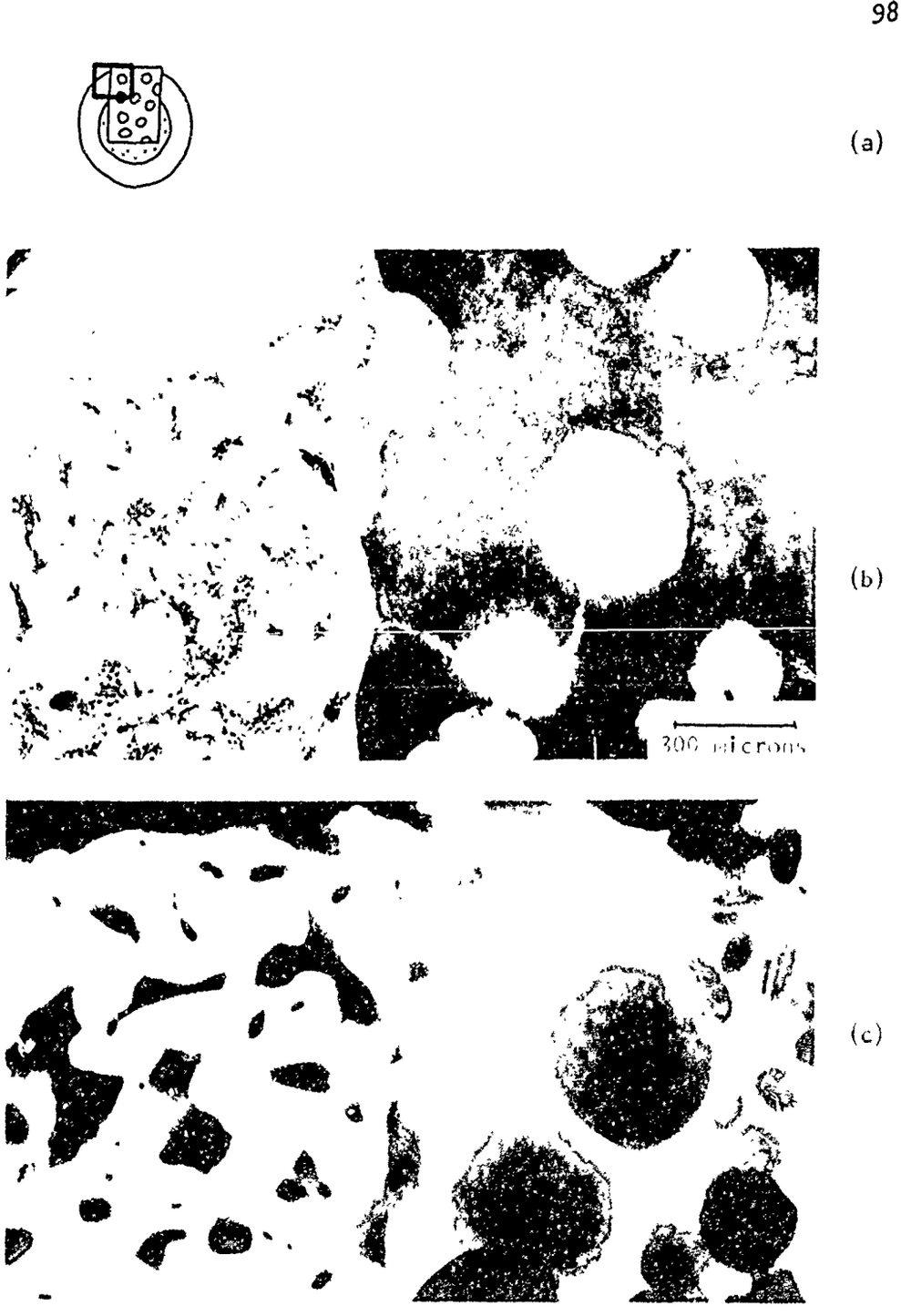

Figure 29. (a) Sketch of a cross section of a tibia from the BILATERAL IMPLANT GROUP with the outlined location of a; (b) photomicrograph, and corresponding [illegible] radiograph demonstrating good osseointegration by bone growth into the aluminum oxide cylinder after 8 weeks.

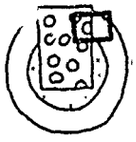

(a)

(b)

Figure 30. (a) sketch of a cross section of the tibia from the BILATERAL IMPLANT GROUP with the outlined location of (b) the photomicrograph demonstrating very good mineralized bone ingrowth into the aluminum oxide pellet after 8 weeks.

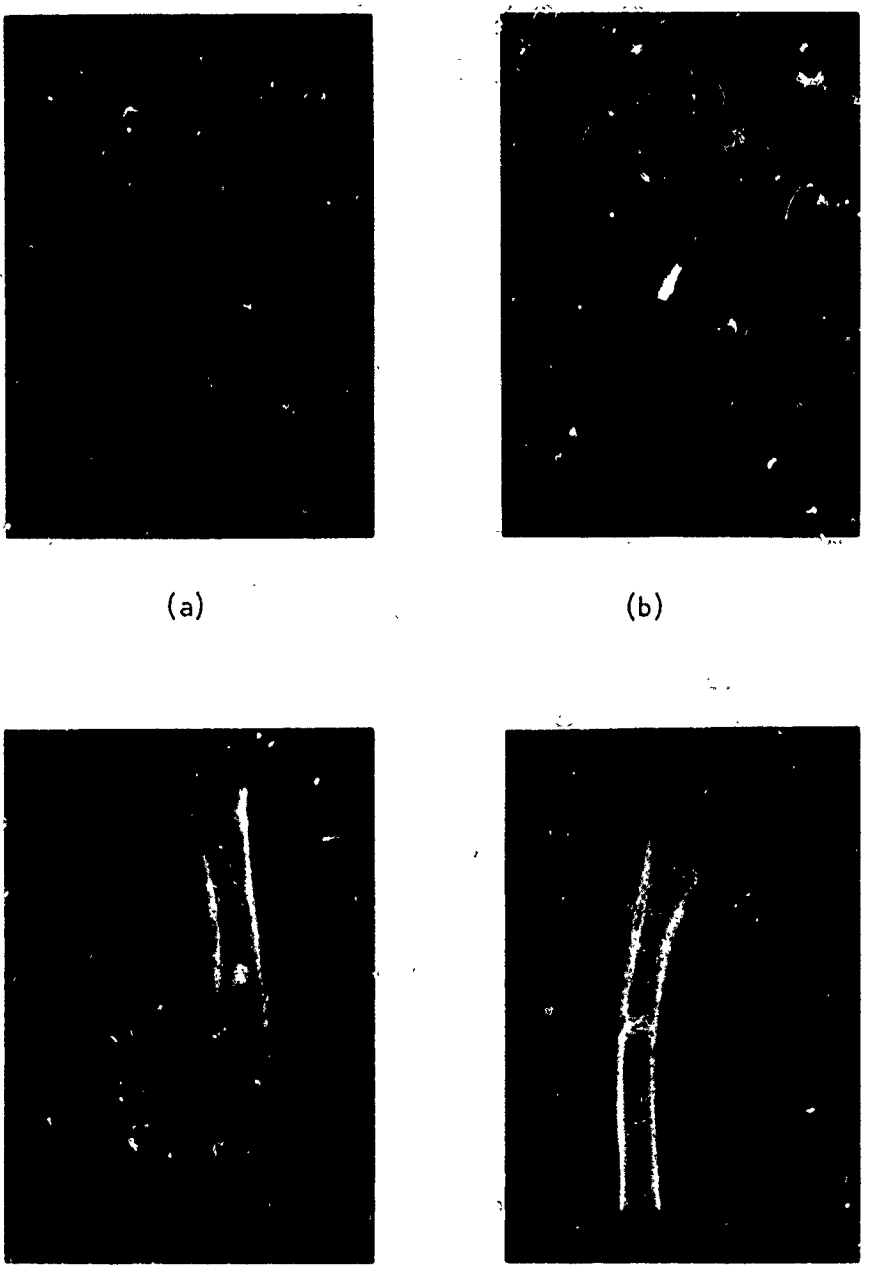

Figure 31. Radiographs of aluminum oxide pellet implants in the right femur of the BILATERAL IMPLANT GROUP: Four week; (a) medio-lateral, (b) anterior-posterior. Eight week; (c) medio-lateral, (d) anterior-posterior.

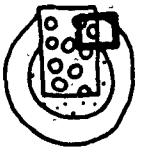

(a)

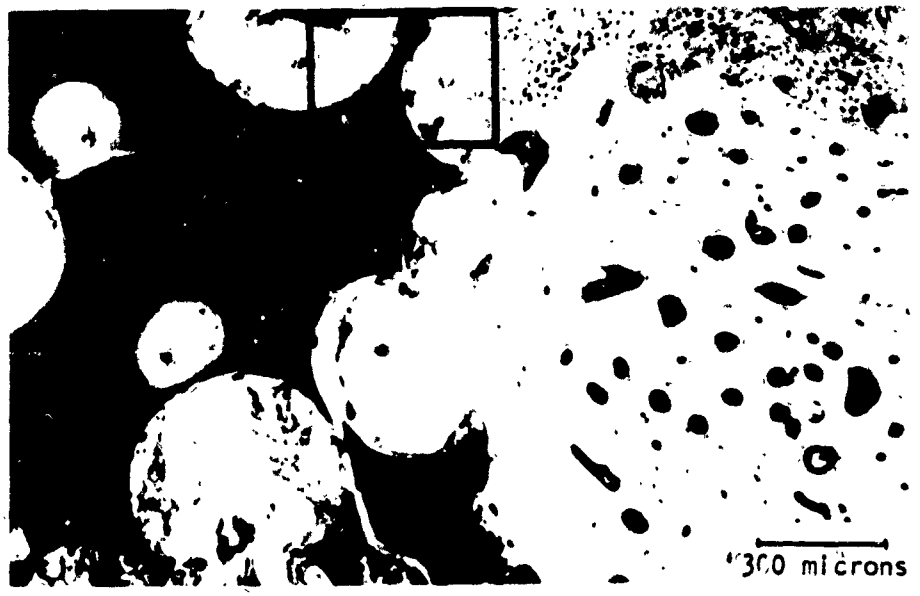

(b)

(c)

Figure 32. (a) Sketch of a cross section of a femur from the BILATERAL IMPLANT GROUP with the outlined location of a: (b) photomicrograph, and corresponding (c) microradiograph demonstrating very good mineralized bone ingrowth into the aluminum oxide pellet after 4 weeks.

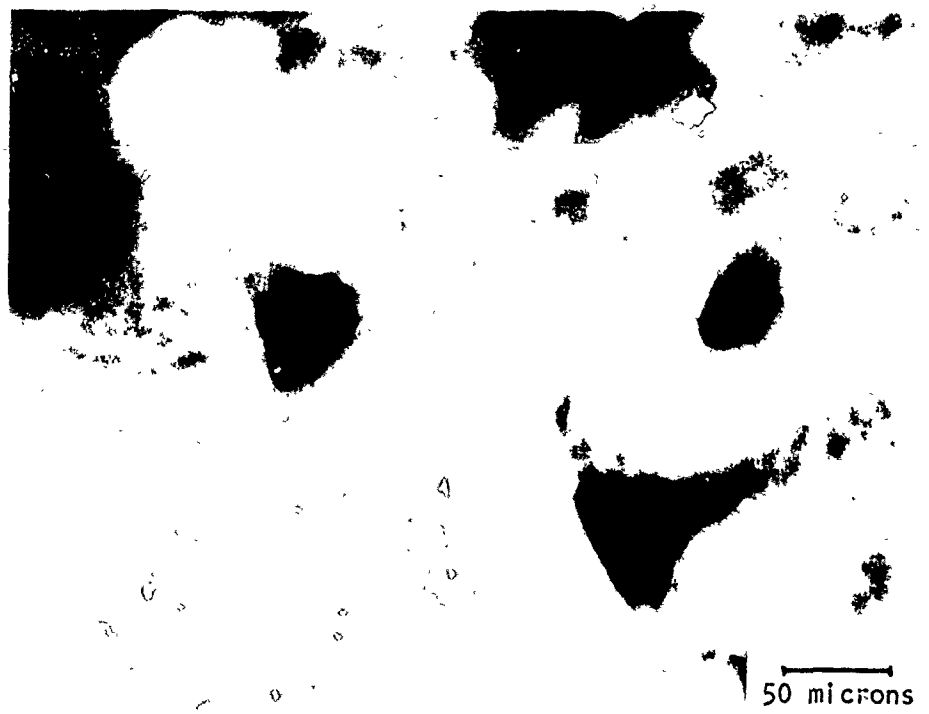

Figure 33. Area outlined in Figure 32 at a higher magnification demonstrating the lack of an osteoid seam.

Inner pores were again well filled with mineralized bone and osteogenic and hematogeneous tissues.

Fibrous connective tissue permeated the surface pores and formed a very thin layer over the exterior of the pellet exposed to the muscle tissues (see Figure 34b). Where pellets protruded past the outer periphery of the cortex, a bony callus formed walling it off from the surrounding soft tissues (see Figure 34c).

The 8 week implants appeared similar to those implanted for 4 weeks except for an almost complete mineralized bone infiltration of surface and internal pores (see Figure 35).

Bilateral Implant Group

Left Tibia - Calcium Aluminate

The results of the post-mortem radiographic analysis indicate no change in the cortical bone of the 4 or 8 week implants outside the periphery of the pellet, which appeared well incorporated into the structure of the tibia. In some 4 week implants a very slight radiotranslucent seam could be seen interjacent to the bone cortex and the implant (see Figure 36). Again, where the tip of the implant fit above or below the periosteum, a callus had formed to incorporate it.

A 4 week histological and microradiologic section demonstrated good mineralized bone ingrowth into surface pores with very limited filling of inner pores (see Figure 37). The ingrowth was hampered by the presence of a separation between the mineralized

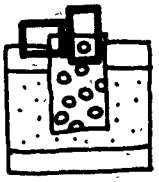

(a)

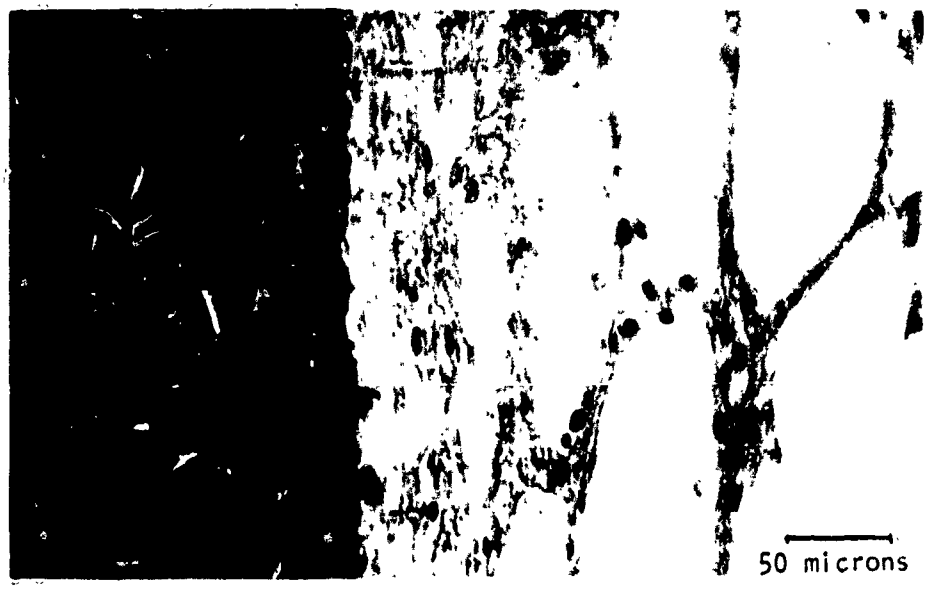

(b)

(c)

Figure 34. (a) Sketch of a longitudinal section of a femur from the BILATERAL IMPLANT GROUP with the outlined location of a; (b) photomicrograph showing encapsulation of exposed aluminum oxide pellet after 4 weeks, and (c) photomicrograph showing bone encapsulation of aluminum oxide pellet protruding past the periosteum of the bone after 4 weeks.

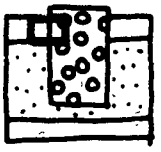

(a)

(b)

(c)

Figure 35. (a) Sketch of a longitudinal section of a femur from the BILATERAL IMPLANT GROUP with the outlined location of a; (b) photomicrograph, and corresponding (c) microradiograph demonstrating excellent mineralized bone ingrowth into the aluminum oxide pellet after 8 weeks.

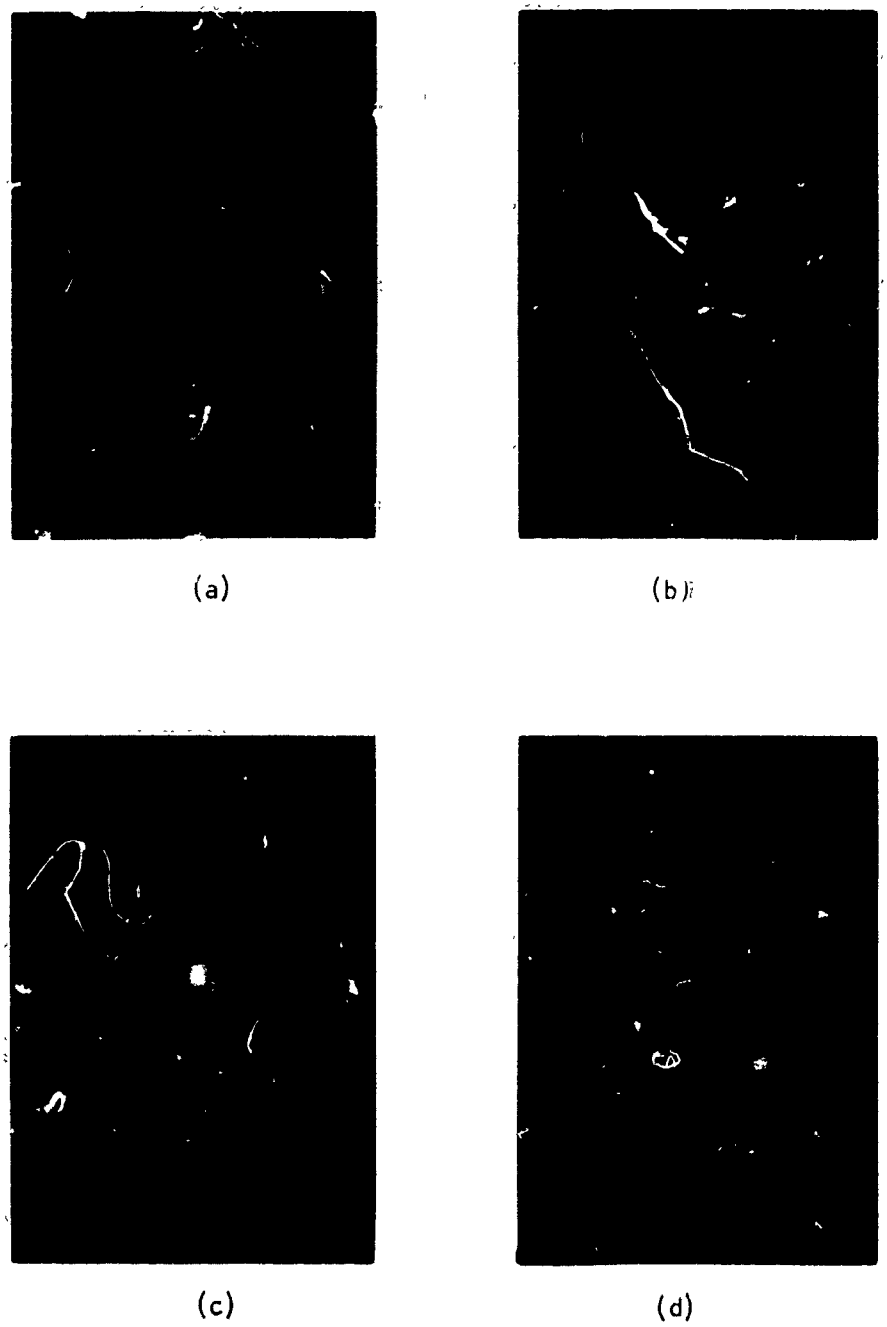

Figure 36. Radiographs of calcium aluminate pellet implants in the left tibia of the BILATERAL IMPLANT GROUP: Four week; (a) medio-lateral, (b) anterior-posterior. Eight week; (c) medio-lateral, (d) anterior-posterior.

(a)

(b)

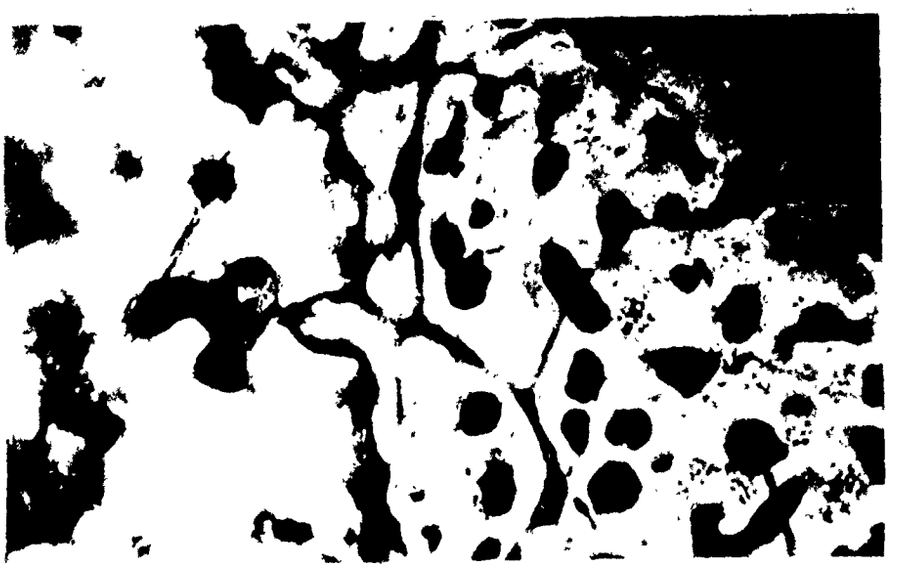

(c)

Figure 37. (a) Sketch of a cross section of a tibia from the BILATERAL IMPLANT GROUP with the outlined location of a; (b) photomicrograph, and corresponding (c) microradiograph demonstrating mineralized bone ingrowth into a calcium aluminate pellet after 4 weeks.

bone ingrowth and the calcium aluminate varying from 10 to 50 microns. The architecture of the bone ingrowth was different from that encountered with aluminum oxide where ingrowth was from the outside to the inside of the pore in that the bone appeared to mineralize from the center towards the periphery. Areas not occupied with mineralized bone were saturated with osteoid, fibrous connective tissue, and hemopoietic tissue.

Calluses which formed over some of the pellets were well affixed to the surface pores of the implant with calcified bone. In many cases where there was a callus present, there was a corresponding increase in the overall porosity of the cortical bone. The cortex of all other implants was completely normal.

The surface pores of the 8 week implants were well infiltrated with mineralized bone as were the internal pores. Again, a 10 to 50 micron seam was noticeable.

Bilateral Implant Group

Left Femur - Calcium Aluminate

The post-mortem radiographs were similar to those for the tibia implants. There was no detectable change in the overall geometry of the femora and in one case where the pellet had protruded a callus had formed. A very thin radiotranslucent area was detected between the calcium aluminate and the cortical bone on a few radiographs (see Figure 38).

The histological and microradiographic sections of the 4 week implants revealed good bone ingrowth, but again a very

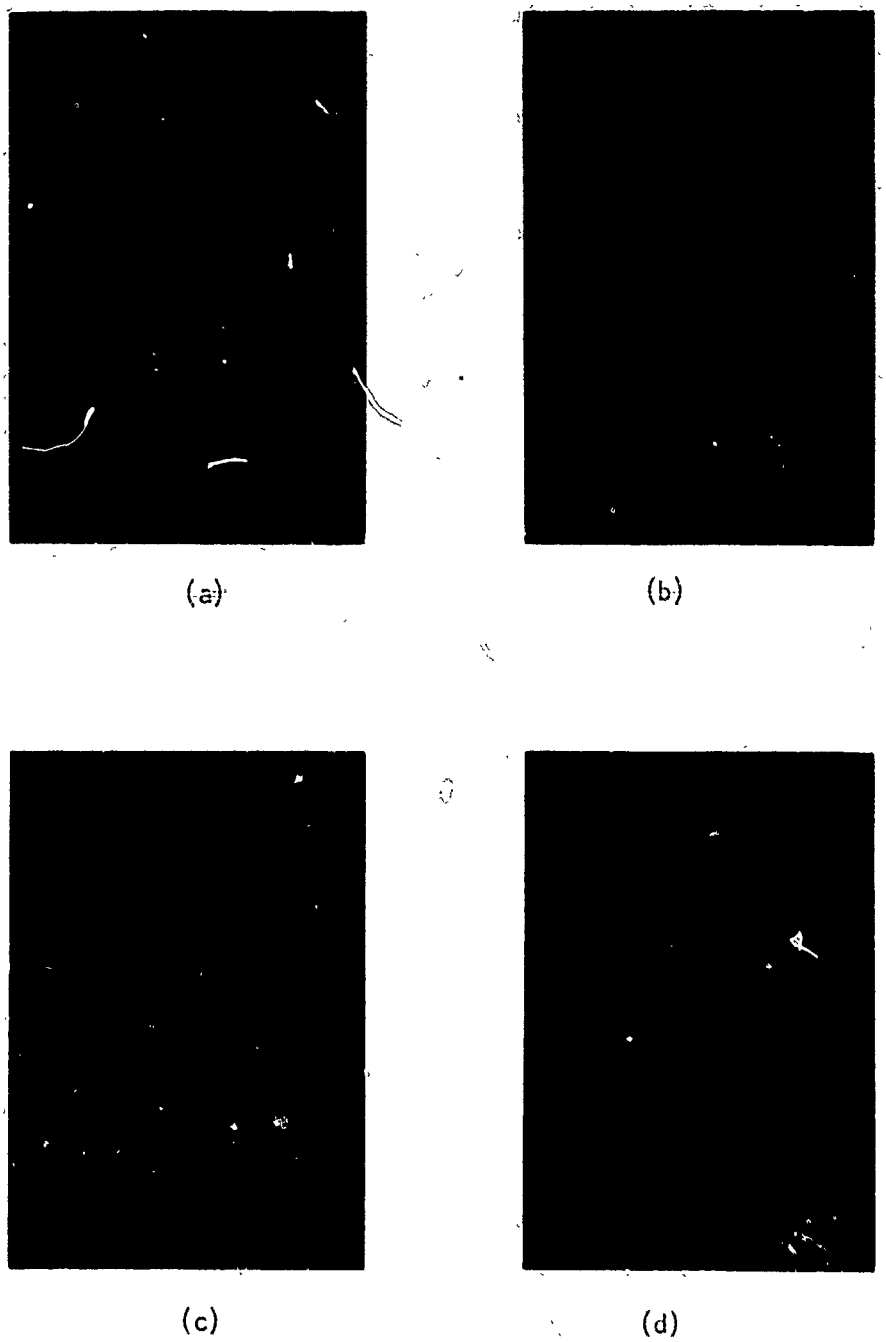

Figure 38. Radiographs of calcium aluminate pellet implants in the left femur of the BILATERAL IMPLANT GROUP: Four week; (a) medio-lateral, (b) anterior-posterior Eight week; (c) medio-lateral, (d) anterior-posterior.

thin seam was detectable separating the mineralized bone and the ceramic (see Figure 39). A bony callus had formed over and into the pellet tips which protruded past the outer periphery of the cortex (see Figure 40).

The 8 week implants demonstrated excellent bone ingrowth into internal and superficial pores, but the seam was still present (see Figures 41 and 42).

Periosteal Scrapes Group

A radiographic analysis of the 4 week amputations where the periosteum was surgically removed from 20 millimeters of the distal end of the tibia indicates that there are 2 bone overgrowths present, one on the tibia and the other on the fibula, located approximately 20 millimeters from the site of amputation and extending up to 10 millimeters radially from the bone shaft. The legs which were injected with the radiopaque media demonstrated increased vascularity in the areas of the spurs when compared to the similarly injected non-amputated limbs (see Figure 43).

There was no visible signs of distal bone overgrowth.

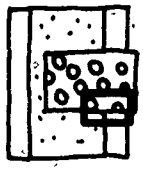

(a)

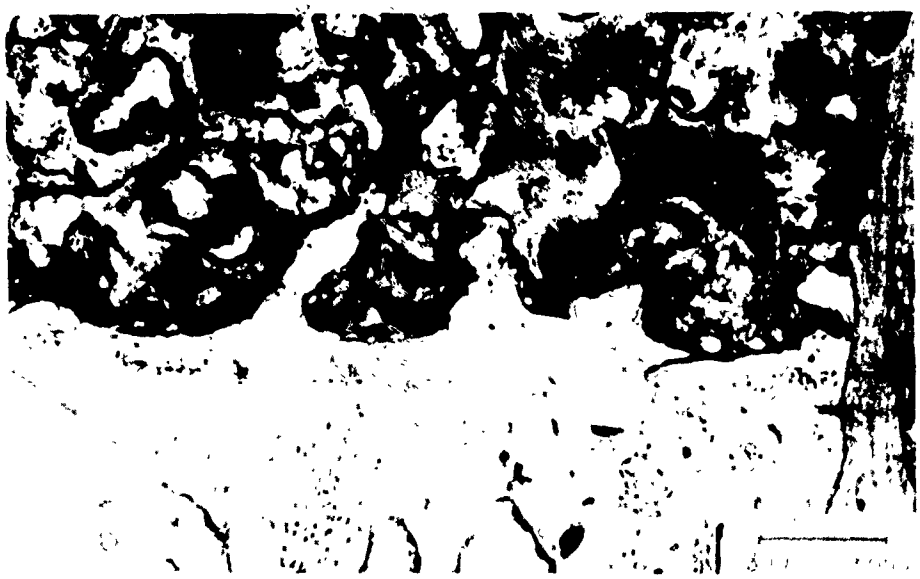

(b)

(c)

Figure 39. (a) Sketch of a longitudinal section of a femur from the BILATERAL IMPLANT GROUP with the outlined location of a; (b) photomicrograph, and corresponding (c) microradiograph demonstrating mineralized bone ingrowth into the calcium aluminate pellet after 4 weeks.

Figure 40. (a) Sketch of a cross section of a femur from the BILATERAL IMPLANT GROUP with the outlined location of a; (b) photomicrograph demonstrating the formation of a bony callus over a calcium aluminate pellet which protruded past the periosteal surface.

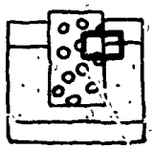

(a)

(b)

(c)

Figure 41. (a) Sketch of a longitudinal section of a femur from the BILATERAL IMPLANT GROUP with the outlined location of a; (b) photomicrograph, and corresponding (c) microradiograph demonstrating mineralized bone ingrowth into a calcium aluminate pellet after 8 weeks.

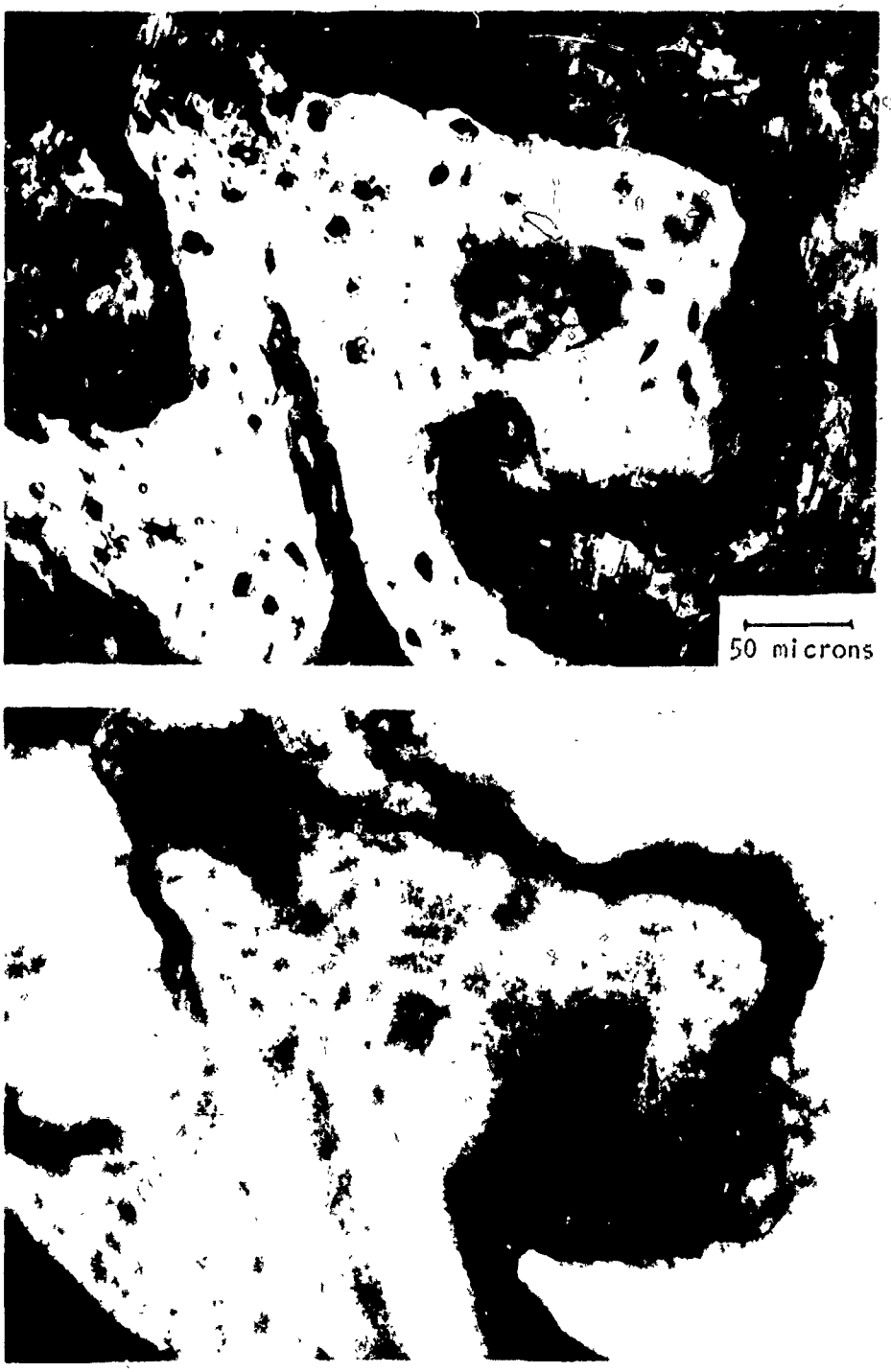

Figure 42. Area outlined in Figure 41 at higher magnifications showing the osteoid seam separating calcium aluminate from mineralized bone.

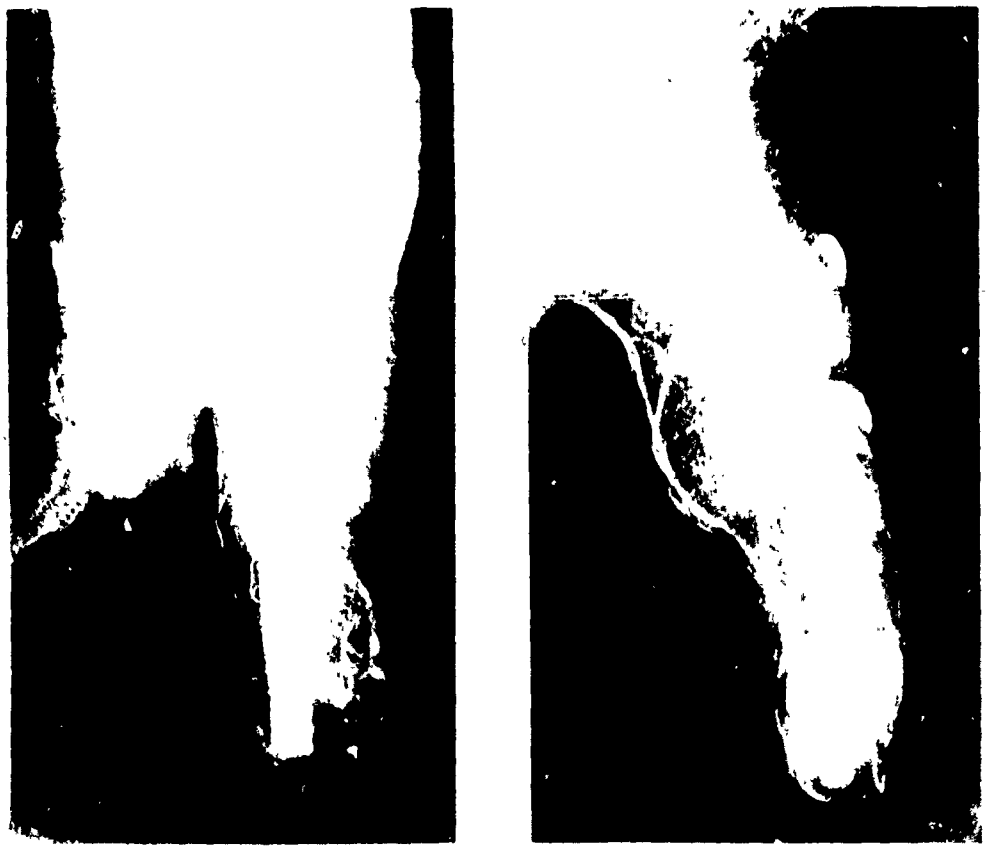

(a) (b)

Figure 43. Radiographs of the left tibia from the PERIOSTEAL SCRAPE GROUP demonstrating the increased vascularity around the bone spur when injected with a radiopaque media after 4 weeks; (a) anterior-posterior, (b) medio-lateral.

CHAPTER VI

DISCUSSION

Material Analysis

The results of the material analysis indicate that the structure of the aluminum oxide implants was highly porous (average value - 62%) and was made up of pore interconnection diameters (55% greater than 100 microns) well within the range reported by Klawitter as necessary for mineralized bone ingrowth (100 microns). The compressive strength of the aluminum oxide implants (average value -3440 psi) was less then than reported by Bowman for calcium aluminate (4100 psi - 51% porous), porcelain (4070 psi - 46% porous), and titanium (4130 psi - 58% porous) implants; but these materials were less porous. For porous aluminate oxide species of 50% porosity, Ryshkewitch[81] reported compressive strengths of approximately 10,000 psi.

In Vivo Testing

The results of the four implant groups--CONE, PELLET, BILATER, and PERIOSTEAL SCRAPES--were compared and interpreted so that the objectives of this research could be answered. Table 4 presents a comparison of the different variables which were qualitatively graded for histologic sections from each type of implant and each time period. The following are the results:

(a) INGROWTH INTO CONE IMPLANTS - the four and eight week Cone implants--CONE IMPLANT GROUP--demonstrated very little

Table 4. Comparison of Histologic Sections.

TYPE IMPLANT	IMPLANT PERIOD	MATERIAL IMPLANTED	MINERALIZED BONE INGROWTH INTO SURFACE PORES	MINERALIZED BONE INGROWTH INTO INNER PORES	CONDITION OF PERIOSTEUM	CONDITION OF ENDOSTEUM
CONE IMPLANT GROUP						
Left Tibia	4 wk	Al_2O_3	0.8	0.8	3.0	3.3
	8 wk	Al_2O_3	1.7	1.2	1.7	1.7
Left Femur	4 wk	Al_2O_3	3.4	0.8	4.7	4.3
	8 wk	Al_2O_3	4.7	2.3	5.0	5.0
PELLET IMPLANT GROUP						
Left Tibia	4 wk	Al_2O_3	2.2	1.3	1.8	2.1
	8 wk	Al_2O_3	3.7	3.0	2.0	2.3
Left Femur	4 wk	Al_2O_3	4.0	2.2	4.6	4.6
	8 wk	Al_2O_3	4.4	2.5	4.2	4.2

Table 4. Comparison of Histologic Sections (cont'd).

TYPE IMPLANT	IMPLANT PERIOD	MATERIAL IMPLANTED	MINERALIZED BONE INGROWTH INTO SURFACE PORES	MINERALIZED BONE INGROWTH INTO INNER PORES	CONDITION OF PERIOSTEUM	CONDITION OF ENDOSTEUM
BILATERAL IMPLANT GROUP						
Left Tibia	4 wk	Ca-Al-O*	4.0	2.5	4.7	4.7
	8 wk	Ca-Al-O*	4.8	3.6	4.5	4.8
Left Femur	4 wk	Ca-Al-O*	3.7	3.3	4.8	4.8
	8 wk	Ca-Al-O*	4.9	4.0	5.0	5.0
Right Tibia	4 wk	Al_2O_3	4.2	3.6	3.9	4.3
	8 wk	Al_2O_3	4.9	3.9	4.0	4.6
Right Femur	4 wk	Al_2O_3	4.6	4.0	4.7	4.9
	8 wk	Al_2O_3	5.0	3.8	5.0	5.0

*20% $CaO \cdot Al_2O_3$

80% $3CaO \cdot 5Al_2O_3$

mineralized bone and osteoid ingrowth into the stem of the implant from the endosteal surface of the tibiae. What was present was a richly vascularized connective tissue with no abnormal inflammatory cells or tissue responses, indicating biological compatibility; but, on the other hand, the implants demonstrated that the conditions were not favorable for the bone to incorporate the implant into the functional structure of the bone. There are two alternative explanations for this: (1) there was insufficient stress being transmitted between the porous aluminum oxide and the tibia necessary to promote bone ingrowth and mineralization, or (2) bone ingrowth perpendicular to the axis of the tibia was biologically and mechanically not possible even if the proper stress conditions did exist. If, in this experiment stress was present, the latter explanation would appear to be appropriate; if not, further research will have to be conducted utilizing an implant design and surgical technique which will provide the proper stress atmosphere to determine if endosteal ingrowth is feasible.

(b) STRESS CONDITIONS - to clearly interpret the overall physiological condition of the amputated limb--PELLET IMPLANT GROUP and CONE IMPLANT GROUP--it was necessary to compare the aluminum oxide pellets in the amputated limbs to corresponding aluminum oxide pellets implanted in an animal without an amputation-BILATERAL IMPLANT GROUP. This was done because it was difficult to distinguish between normal bone remodeling where there is some porosity and vascularity of the periosteum as is expected in 3 to 5 month old rabbits at an intermediate stage of

bone ingrowth (74) and abnormal conditions such as osteoporosis where bone resorption and growth rates are also changing but to a far greater extent.

The 4, and to a far greater extent, 8 week pellet implants in the non-amputated tibiae and femora--BILATERAL IMPLANT GROUP--showed almost complete mineralized bone ingrowth into surface pores and an almost thorough permeation of inner pores. The pellets were well incorporated into the bone structure. The cortical bone of the tibiae and femora were, on the whole, void of porotic areas other than the normally expected number of Haversian systems which were in the stages of being renewed and reconstructed. A layer of specialized osteogenic connective tissue characterized the normal periosteum and endosteum.

The 4 and 8 week pellet implants in the femora of the amputated limbs--PELLET IMPLANT GROUP--demonstrated slightly less ingrowth than the corresponding non-amputated femora along with an increase in the presence of periosteal and endosteal bone porosity characteristic of mild disuse osteoporosis. The difference in porosity between the amputated and non-amputated femora was caused by the animal's tendency not to apply weight to the amputated limb.

The aluminum oxide pellet implants in the tibiae--PELLET IMPLANT GROUP--where the musculature was disturbed demonstrated a great deal less mineralized bone ingrowth into the surface and inner pores when compared to similar Al_2O_3 implants in the tibiae of non-amputated limbs--BILATERAL IMPLANT GROUP. The overall geo-

metry of the cortical bone around the tibiae implants showed distinct signs of disuse osteoporosis characterized by the presence of periosteal resorption and an overall thinning of the cortical bone. The change was caused by lack of weight bearing and damage to muscle action.

Examination of the histologic sections and additional radiographs of the amputated limbs which had been injected with a radiopaque media (PERIOSTEAL SCRAPES) showed that porosity was much more severed towards the distal end of the tibia where there was hypervascularity, extensive periosteal resorption, and a greatly increased porosity in the cortical bone. These changes were associated with a lack of stress in the form of body wieght from the disruption of the normal musculature whose contractures play an important role in bone physiology and the changes in the vascular network.

(c) BIOCOMPATIBILITY OF ALUMINUM OXIDE - a gross examination of necropsy of the tissues surrounding each implant indicated that there was no abnormal tissue reactions to the aluminum oxide or calcium aluminate.

Further histologic analysis of all aluminum oxide sections indicated no signs of abnormal carcinogenic, allergenic, immunologic, or inflammatory response present. The material's chemical stability and non-toxicity were further supported by the lack of any osteoid or other tissue seam where the mineralized bone juxtaposed the aluminum oxide. The remaining pore areas were permeated with normal hemopoietic and connective tissues.

The excellent mineralized bone ingrowth into surface and inner pores of the 4 and 8 week aluminum oxide implants in non-amputated limbs--BILATERAL IMPLANT GROUP--demonstrate that with habitual weight bearing, undamaged musculature, and normal vascularity there was excellent mechanical compatibility with both cortical bone and surrounding soft tissues.

On the other hand, the calcium aluminate sections demonstrated the presence of a 10 to 50 micron osteoid seam which separated mineralized bone from the ceramic. Klawitter (56) reported a similar seam and hypothesized that it was caused by surface hydration of the calcium aluminate interfacing with the bone mineralization.

The authors felt that it was particularly important to note that sections from all aluminum oxide pellet implants demonstrated interconnected bone spicules lining the internal pores of the implant which lay in the bone marrow area (see Figure 44). This may indicate that the structure and composition of the porous aluminum oxide implants favorably affected bone deposition and mineralization.

(d) BONE SPURS - radiograph made at necropsy of the tibiae of the PERIOSTEAL SCRAPE GROUP indicated that the origin of the two opposing bone spurs was approximately 15 millimeters proximal to the site of the original amputation to which the periosteum had been originally stripped. This supports the hypothesis that surgical irritation to the periosteum is one cause of bone spurs.

The vascular networks of the limbs into which a radiopaque media had been injected indicated an increased vascularity incom-

Figure 55. Microradiograph [illegible] [illegible] [illegible] network of bone spicules throughout the [illegible] fracture [illegible] [illegible]

passing the site of the bone spur and not present at the extreme distal tip of the tibia. This may be associated with the body's attempt to meet the higher blood demands where spurs develop or it might be part of a vast network which formed to bridge the ligated arteries to veins.

CHAPTER VII

CONCLUSIONS

1. The pore structure of the aluminum oxide implant material was suitable for mineralized bone ingrowth.

2. There was little mineralized bone ingrowth into the cone shaped aluminum oxide implants in the distal tip of the amputated tibia.

3. Aluminum oxide pellet implants in the tibiae or femora of the amputated limbs showed very good calcified bone growth into surface and internal pores, but it was not complete for an implant resident time of eight weeks.

4. The excellent mineralized bone ingrowth into surface and internal pores of the aluminum oxide pellets in the tibiae and femora of the non-amputated limbs demonstrated that the incomplete mineralized bone ingrowth into similar pellets in amputated limbs was related to a lack of weight bearing and damage to the musculature and vascularity following amputation.

5. Calcium aluminate pellet implants in the tibiae and femora of non-amputated limbs demonstrated less ingrowth than corresponding aluminum oxide implants. The calcium aluminate demonstrated the presence of an osteoid seam.

6. The aluminum oxide implants were observed to be non-toxic and elicited no inflammatory responses.

7. There was little or no osteoid seam separating the aluminum oxide implants and mineralized bone.

8. Bone spurs, one on the medial surface and one on the lateral surface of the amputated tibiae, originated at the site where the periosteum was damaged and was associated with an increase in the vascularity of the adjacent tissues.

LITERATURE CITED

1. Aga, V. June 1970. Preparation of Undecalcified Bone Sections. The Indian Journal of Medical Science. 24:361-365.

2. Aitken, G. T. Sept. 1962. Overgrowth of the Amputation Stump. Inter-Clinic Bulletin. 1(11):1-8.

3. Aitken, G. T. May 1968. The Child with an Acquired Amputation. Inter-Clinic Information Bulletin. 7(8):1-15.

4. Allen, A. C. May 1967. CerCom Insulates Space Crafts. Ceramic Industry Magazine. :52-54.

5. ASTM. 1963. Compressive Strength of High-Strength Ceramic Materials. ASTM Designation C528-63T:320-322.

6. Anderson, L. D., W. R. Hamsa and T. L. Waring. July 1964. Femoral Head Prostheses. Journal of Bone and Joint Surgery. 46A(5):1049-1065

7. Arden, G. P., A. R. Taylor and B. M. Ansell. 1970. Total Hip Replacement Using the Mckee-Farrar Prosthesis. Ann. Rheum. Dis. 29(1):1-5.

8. Beder, O. E., G. Eade. 1956. An Investigation of Tissue Tolerance to Titanium Metal Implants in Dogs. Surgery. 39:470-473.

9. Bleicher, N. Mar. 1960. Preoperative and Postoperative Care of the Laboratory Dog. Proceedings of the Animal Care Panel. 10(1):5-24.

10. Bowman, L. S. 1971. Characterization of Tissue Growth into Pellets and Partial Sections of Porous Ceramics Implanted in Bone. M.S. Thesis. Clemson University, Clemson, South Carolina.

11. Brooks, M., A. C. Elkin, R. G. Harrison and C. B. Heald. 1961. A New Concept of Capillary Circulation in Bone Cortex. Some Clinical Applications. Lancet. 1:1078-1081.

12. Burwell, H. N. Sept. 1967. Replacement of the Femoral Head by a Prosthesis in Subcapital Fractures. British Journal of Surgery. 54(9):741-749.

13. Charnley, J. Aug. 1964. The Bonding of Prostheses to Bone by Cement. J. Bone Joint Surgery. 46B(3):518-529.

14. Charnley, J. Dec. 1967. Total Prosthetic Replacement of the Hip. Physiotheraphy. 53:407-409.

15. Charnley, J., F. Follacci and B. T. Hammond. 1968. Long-term Reaction of Bone to Self-Curing Acrylic Cement. J. Bone Joint Surgery. 50B(4):822-829.

16. Charnley, J. 1960. Anchorage for the Femoral Head Prosthesis to the Shaft of the Femur. J. Bone Joint Surgery. 43B:28-30.

17. Cohen, J. June 1966. Performance and Failure in Performance of Surgical Implants in Orthopedic Surgery. J. Materials. 1(2):354-365.

18. Cohen, J. and G. Hammond. 1959. Corrosion in a Device for Fracture Fixation. J. Bone Joint Surgery. 41A:524-534.

19. Crabbe, W. A. 1968. Rheumatoid Arhtritis Affecting the Hip. Guy. Hosp. Rep. 117:31-47.

20. Curran, R. C. 1966. Color Atlas of Histopathology. Oxford Univer. Press. New York. Pg. 94.

21. Danckwardt-Lilliestrom, Goran. 1969. Reaming of the Medullary Cavity and Its Effect on Diaphyseal Bone. Acta Orhtopaedica Scandinavica Supplementum No. 128. Munksgaard, Copenhagen.

22. Drake, L. C. and H. L. Ritter. 1945. Macropore-Size Distributions in Some Typical Porous Substances. Industrial and Engineering Chemistry. 17(12):787-791.

23. Erikson, U. 1965. Circulation in Traumatic Amputation Stump. Acta Radiologica Suppliment 238. 122 pages.

24. Erikson, U. 1966. Healing of Amputation Stumps, With Special Reference to Vascularity and Bone. Acta Orthopaedica Scandinav. 37:20-28.

25. Esslinger, J. O. A Basic Study in Semi-Buried Implants and Osseous Attachments for Application to Amputation Prosthetic Fitting. Personal Copy.

26. Esslinger, J. O. Highlights of VA Contractual Research Program--Prosthetics. Personal Copy.

27. Flax, M. H. and J. B. Caulfield. Oct. 1962. Use of Methacrylate Embedding in Light Microscopy. 74:137-145.

28. Froysaker. 1968. The Thompson Prosthesis in Femoral-Neck Fracture, Non-union and Avascular Necrosis of the Head of the Femur. Acta Chir. Scand. 134:119-123.

29. Galante, J., R. Lueck and W. Rostoker and R. D. Ray. Jan. 1971. Sintered Fiber Metal Composites as a Basis for Attachment of Implants in Bone. J. Bone Joint Surgery. 53-A(1):101-114.

30. Gelb, J. 1965. Lecture, Kessler Institute. Newark, New Jersey.

31. Golden, G. T. Apr. 1969. The Use of Prosthetics in Surgery of the Hip. North Carolina Med. J. 30:135-142.

32. Haboush, E. J. 1953. A New Operation for Arthroplasty of the Hip Based on Biomechanics, Photoelasticity, Fast-Setting Dental Acrylic, and Other Considerations. Bull. of the Hospital for Joint Diseases. 14(2):242-277.

33. Hager, J. E. 1968. Limb Prosthetics. Hager Prosthetics, Inc., Columbia, South Carolina.

34. Hall, C. W., R. H. Eppright and T. Engen and D. Liotta. 1967. A Permanently Attached Artificial Limb. Trans. Amer. Soc. Artif. Int. Organs. 13:329-331.

35. Heikel and V. A. Henrik. 1960. On Ossification and Growth of Certain Bones of the Rabbit; With a Comparison of the Skeletal Age in the Rabbit and in Man. Acta Orth. Scand. 29(3):171-184.

36. Held, A. J. and M. Spirgi. Apr. 1968. Osteoperiostal Response to Various Implants in Rabbits. Helv. Odent. Acta. 12(1):1-14.

37. Hench, L. L. Aug. 1970. An Investigation of Bonding Mechanisms at the Interface of a Prosthetic Material. Report No. 1. Personal Copy. 61 pages.

38. Hentrich, R. L. and G. A. Graves. 1971. An Evaluation of Inert and Resorbable Ceramics for Future Clinical Orthopedic Applications. J. Biomed. Mat. Res. 5:25-51.

39. Hill, J. T. and J. C. Eaton and H. G. Mouhot and F. Leonard. 1967. Porous Plastic Prostheses. J. Biomed. Mater. Res. 1:253-261.

40. Hinchey, J. J. 1964. Primary Prosthetic Replacement. J. Bone Joint Surgery. 46-A:223-244.

41. Hirschhorn, J. S. and J. T. Reynolds. Powder Metallurgy Fabrication of Cobalt Alloy Surgical Implant Materials. University of Wisconsin. Pg. 137-150.

42. Homsey, C. A. Personal communication, Clemson University, 1971.

43. Houck, C. E. and E. W. Dempsey. July 1954. Cytological Staining Procedures Applicable to Methacrylate-Embedded Tissues. Stain. Tech. 29(4):207-211.

44. Hulth, A. May 1962. Studies in Amputation Stumps in Rabbits. J. Bone Joint Surgery. 44-B(2):431-435.

45. Jaffe, H. L. and M. M. Pomeranz. 1934. Changes in the Bones of Extremities Amputated Because of Arteriovascular Disease. Arch. of Surgery. 29:566-588.

46. Jenkins, D. P. and T. H. Cochran. May-June 1969. Osteoporosis: The Dramatic Effect of Disuse of an Extremity. Clinical Orthopaedics and Related Research. 64:128-134.

47. Jennings, B. M. and M. G. Farquhar and H. D. Moon. 1959. Staining Methods for Osmium-Methacrylate Sections. Am. J. Path. 35:991-997.

48. Jowsey, J. 1965. Quantitative Microradiographic Studies of Normal and Osteoporotic Bone. J. Bone Joint Surgery. 47-A(4):785-806.

49. Judet, J. and R. Judet. 1950. The Use of an Artificial Femoral Head for Arthroplasty of the Hip Joint. J. Bone Joint Surgery. 32-B:166.

50. Kelly, P. J. June 1968. Anatomy, Physiologg, and Pathologv of the Blood Supply of Bones, J. Bone Joint Surgery. 50-A(4):766-783.

51. Kelly, P. J. and J. M. Janes and L. F. Peterson. Sept. 1959. The Effect of Arteriovenous Fistulae on the Vascular Pattern of the Femora of Immature Dogs. J. Bone Joint Surgery. 41-A:1101-1108.

52. Kelly, P. J. and J. Jowsey and L. Riggs. 1965. A Comparison of Different Morphologic Methods of Determining Bone Formation. Clinical Orthopaedics and Related Research. 40:7-11.

53. Kingery, W. D. 1967. Introduction to Ceramics. John Wiley and Sons, Inc. New York. Pages 412-417.

54. Kirk. N. T. 1944. The Development of Amputation. Bull. of Med. Library Assoc. 32:132-163.

55. Klawitter, J. J. 1970. A Basic Investigation of Bone Growth into a Porous Ceramic Material. Ph.D. Thesis. Clemson University, Clemson, South Carolina.

56. Klawitter, J. J. 1971. Research Techniques in Bio-Evaluation of Hard Material Implants. Workshop on Research Techniques in Biomaterials Evaluation. Clemson University, Clemson, South Carolina.

57. Laing, P. E. July 1958. The Significance of Metallic Transfer in the Corrosion of Orthopaedic Screws. J. Bone Joint Surgery. 40-A.

58. Laing, P. G. 1953. The Blood Supply of the Femoral Shaft. J. Bone Joint Surgery. 35-B:462-466.

59. Lambert, C. N. June 1966. A Different Viewpoint on Overgrowth. Inter-Clinic Information Bulletin. 5:15-16.

60. Larson, R. L. and P. J. Kelly and J. M. Janes. 1961. Suppression of the Periosteal and Nutrient Blood Supply of the Femora of Dogs. Clinical Orthop. and Related Research. 21:217-225.

61. Leonard, R. 1971. Personal Consultation. Clemson Univ., Clemson, South Carolina.

62. Luft, J. H. 1961. Improvements in Epoxy Resin Embedding Methods. J. Biophysich. and Biochem. Cytology. 9:409-414.

63. Lulu, D. J. June 1969. Femoral Head Prostheses: Thirteen Year's Experience. The Amer. Surgeon. 35(6):418-421.

64. Mazet, R. Dec. 1968. Syme's Amputation. J. Bone Joint Surgery. 50-A(8):1549-1563.

65. McMaster, P. E. and W. C. Boeck. Nov.-Dec. 1964. Concepts and Cases in Amputation Surgery. Clinical Orthopaedics and Related Research. 37:32-31.

66. Miller, I. and J. E. Freund. 1965. Probability and Statistics for Engineers. Prentice-Hall, Inc., New Jersey. Pages 117-118.

67. Moodie, R. L. 1923. Paleopathology: An Introduction to the Study of Ancient Evidences of Disease. Univ. of Illinois Press, Urbana. Page 532.

68. Mooney, V. and M. Heppenstall and W. Knapp. 1969. Direct Skeletal Attachment of an Artificial Limb. Paper Presented at the Symposium on "Use of Ceramics in Surgical Implants". Clemson Univ., Clemson, South Carolina.

69. Mooney, V. Personal communication, Clemson University. 1971.

70. Moore, A. T. 1957. The Self Locking Metal Hip Prosthesis. J. Bone Joint Surgery. 39-A:811.

71. Morrison, S. J. 1971. Tissue Reaction to Three Ceramics of Porous and Non-porous Structures. M.S. Thesis. Clemson Univ., Clemson, South Carolina.

72. Nelson, G. E., Jr. and P. J. Kelly and L. F. Peterson. June 1960. Blood Supply of the Human Tibia. J. Bone Joint Surgery. 42-A:625-636.

73. Nordby, E. J. and K. M. Sachtien. Mar.-Apr. 1968. Femoral Head Prosthesis for Hypertrophic Arthritis of the Hip. Clin. Orthop. 57:191-202.

74. Owens, M. and J. Jowsey and J. Vaughan. May 1955. Investigation of the Growth and Structure of the Tibia of the Rabbit by Microradiographic and Autoradiographic Techniques. J. Bone Joint Surgery. 37-B(2):324-342.

75. Peterson, L. T. Mar. 1967. Hip Prosthesis for Fracture of the Femoral Neck. Med. Ann. D.C. 36:159-162.

76. Ring, P. A. Nov. 1968. Complete Replacement Arthroplasty of the Hip by the Ring Prosthesis. J. Bone Joint Surgery. 50-B(4):720-731.

77. Rivkurd, L. E. July 1967. Improved Technology for Rigid Inorganic Foams. The Journal of Cellular Plastics. Pages 3-7.

78. Robbins, S. L. Oct. 1969. Pathology. W. B. Saunders, Co., Philadelphia. Pg. 1333-1334.

79. Romano, R. L. and E. M. Burgess. Jan. 1966. Extremity Growth and Overgrowth Following Amputation in Children. Inter-Clinic Information Bulletin. 5:11-12.

80. Ross, G. and L. Smith. 1969. Paper presented at: A Symposium on Use of Cermaics in Surgical Implants. Clemson Univ., Clemson, South Carolina.

81. Ryshkewitch, E. Feb. 1968. Compression Strength of Porous Sintered Alumina and Zirconia. J. Amer. Ceramic Society. 36(2):65-68.

82. Sarmiento, A. and H. A. Grimes. 1963. The Use of the Austin T. Moore Vitallium Prosthesis in the Treatment of Acute Fractures and Other Diseases of the Hip. Clinical Orthop. and Related Research. 28:120-131.

83. Scales, J. T. and G. D. Winter and H. T. Shirley. Nov. 1959. Corrosion of Orthopaedic Implants. J. Bone Joint Surgery. 41-B(4).

84. Sevastikoglou, J. A. and U. Erikson and S. E. Larsson. 1969. Skeletal Changes of the Amputation Stump and Femur on the Amputated Side. Acta Orthop. Scandinav. 40:624-633.

85. Smith, L. Oct. 1963. Ceramic-Plastic Material as a Bone Substitute. Archives of Surgery. 87:653-661.

86. Spurlock, B. D. and M. S. Skinner and A. A. Kattine. 1966. A Simple Rapid Method for Staining Epoxy-Embedded Specimens for Light Microscopy with Polychromatic Stain Paragon--1301. The Amer. Jour. Clin. Path. 46(2): 252-258.

87. Stinchfield, F. E. and B. Cooperman and C. E. Shea. Oct. 1957. Replacement of the Femoral Head by Judet or Austin Moore Prosthesis. J. Bone Joint Surgery. 39-A:1043-1058.

88. Swanson, A. B. Bone Overgrowth in the Juvenile Amputee and Its Control by the Use of Silicone Rubber Implants. Personal Copy.

89. Swanson, A. B. Mar. 1965. Phocomelia and Congenital Limb Malformation--Surgical Reconstruction and Prosthetic Replacement. Amer. J. Surg. 109:294-299.

90. Swanson, A. B. Feb. 1966. Improving End-bearing Characteristics of Lower Extremity Amputation Stumps--A Preliminary Report. Inter-Clinic Information Bulletin. 5:1-7.

91. Talbert, C. D. 1969. A Basic Investigation into the Potential of Ceramic Materials as Permanently Implantable Skeletal Prostheses. M.S. Thesis. Clemson Univ., Clemson, South Carolina.

92. Thompson, F. R. June 1954. Two and a Half Year's Experience With a Vitallium Intramedullary Hip Prosthesis. J. Bone Joint Surgery. 36-A(3):489-502.

93. Thomson, J. E. M. Jan. 1952. A Prosthesis for the Femoral Head; A Preliminary Report. J. Bone Joint Surgery. 34-A(1):175-182.

94. Turek, S. L. 1967. Orthopaedics--Principles and Their Applications. J. B. Lippincott Co., Toronto. Pg. 687-693; pg. 962-964.

95. Ulmer, G. C. and W. T. Smothers. 1967. Application of Mercury Porosimetry to Refractory Materials. Ceramic Bulletin. 46(7):649-652.

96. Von Saal, F. 1943. Amputations in Children. Surgery, Gynecology, and Obstetrics. 1:708.

97. Weast, R. C. 1969. Handbook of Chemistry and Physics. The Chemical Rubber Co., Cleveland, Ohio.

98. Weiss, M. Feb. 1966. The Prosthesis on the Operating Table from the Neurophysological Point of View. Report of Workshop Panel on Lower-Extremity Prosthetic Fitting. Committee on Prosthetics Research and Development, National Academy of Science.

99. Westerman, R. E. 1971. Personal Consultation, Clemson, South Carolina.

100. Wilson, A. B., Jr. Apr. 1967. Limb Prosthetics--1967. Artificial Limb. 11:1-46.

101. Young, J. F. Feb. 1970. Effect of Organic Compounds on the Interconversions of Calcium Aluminate Hydrates: Hydration of Tricalcium Aluminate. J. Amer. Cer. Soc. 53(2):65-69.

102. Zaccalini, P. S. and R. V. Marshall. 1964. Traumatic Periosteal Proliferations in Rabbits. Journal of Trauma. 4:344-357.

APPENDIX

AMPUTATION COMPLICATIONS

The amputation stump is often plagued with abnormal bone growths, infection, edema, muscle and skin contracture, hemorrhage, and the Phantom Limb syndrome. The presence of any of these will seriously hinder the success of the patient's recuperation and rehabilitation.

Immediate treatment of excessive post-surgical hemorrhage from either minor vessels or from a massive ligature failure is essential (65,94). Minor bleeding should be stopped by first aspirating the wound followed by the application of a pressure bandage. If this is not done, scarring and infection may follow. Large bleeders must be religated to prevent excessive blood loss. In either case a stump which does not properly heal will ulcerate when a prosthesis is applied (94).

Poor surgical technique can cause infection either superficially, localized internally, or at the bone. Superficial infections cause the skin to atrophy, and this may be followed by sloughing (65). Hot packs, chemotherapy, antiobiotics and elevation of the stump are the prescribed treatment. In the case of an internal infection the skin must be reopened so that any foreign body can be removed and the wound drained. Bone infections require that a sequestrectomy and surgical repair be performed.

Proper fitting of the prosthesis is extremely important. In cases where there is not a good mating of the surfaces between

prosthesis and stump, an uneven force distribution over the stump will cause edema (33, 100). If this is not remedied, ulcers will form which are very painful. The stump must then have special treatment to control infection and allow the skin to return to normal. The remaining scar must be removed down to normal tissue so that the skin can be reclosed and a new prosthesis fitted (94).

Muscle and skin contracture are caused by inactivity of the tissues and diminished blood supply which are a direct result of either poor surgical technique or improper post-surgical limb care (79,65,100). Since bone does not diminish in length significantly as muscle and skin do, the latter must be amputated at a lower level to compensate for this difference. Contracture are also reduced by applying a tightly bound dressing immediately following surgery, as discussed previously. If excessive contracture does occur, the bone can become exposed, resulting in infection and a need for a complete stump revision.

The Phantom Limb sensation usually appears in early post-operative phases of rehabilitation and then gradually fades away. In only a very few amputees does this continued sensation of the lost limb create a significant enough problem to require medication for relief. The occurrance of this symptom can be minimized by careful handling of the tissues, especially nerves, during surgery (65).

Abnormal bone growth occurs in many amputations because of either damage to the periosteum, change in blood supply, or change

in force direction and/or magnitude in the bone. The 3 main abnormalities are spur formation, axial bone overgrowth, and osteoporosis.

Spurs have been described as periosteal proliferations along the cortical shaft of long bones directed away from the force axis of the bone (44). There are many theories concerning the cause of the spurs. Erikson (23,65,24), following a study of the occurrance of spurs on amputated rabbit tibiae, described the oxotosis as arising from either a hematoma or a tissue change in the area accompanied by increased vascularity. His decision was based on numerous radiographs of bones whose vascular systems had previously been injected with a radiopaque media. Zaccalini (102) produced similar spurs in rabbits by dropping a 420 gram hammer on each thigh, indicating that the blow damaged the periosteum enough to initiate proliferation. In an attempt to produce corresponding results by surgically stripping the periosteum, he found that this occurred when geletin or plastic sponge was wrapped around the cortex. This is not in agreement with McMaster (65) who found that spurs formed when the bone was left rough at the end following surgical amputation in humans.

The problem of bone overgrowth following traumatic amputation has been reported by many (21,25,26,59,79,88,90). At the Area Child Amputee Center in Grand Rapids, Michigan the incidence of bone overgrowth was reported by Swanson as 12.4 percent of 314 patients (45). It has also been reported by Von Seal (96) that 16 of 20 juvenile below-knee amputees had either bone protrusion or

painful stumps caused by tightly stretched skin or spurs protruding from the bone. It is important to recognize that this is a problem only in juvenile amputees, for when the epiphyses close with skeletal maturity, the tendency towards bone overgrowth becomes insignificant (3).

The actual cause of overgrowth is not very well understood. It has been noted by Gelb (30), for instance, that an inadequate skin covering over the stump can create an overgrowth problem. The tightness of the skin puts pressure on the bone stump which stimulates additional growth. Roman and Burgess (79) explain the problem from a circulatory viewpoint. It is their opinion that the circulation to the proximal epiphysis is not damaged by amputation so the bone continues to grow normally whereas the soft tissue, because of muscle atrophy and diminished blood supply, loses its potential to grow at the same rate that bone does. This results in physical irritation followed by stump protrusion through the muscle and skin. Additional work by Esslinger (25) showed that damage to either the periosteum or the endosteum during surgery will result in the formation of a ring sequestrum. This also seems to be a logical theory; for when an area of bone is damaged, as with a fracture, a repairative growth process is initiated.

Regardless of which theory is correct, once the appositional growth (88) has begun, the problem becomes self-propagating. The additional bone stretches the skin which increases pressure on the bone, and so on. Fibrosis and adhesion of the soft tissue to the bone also becomes evident. This finally leads to inflammation and

ulceration of the skin followed by protrusion of the bone through the skin permitting chronic infection (89,79). When this occurs, revision of the stump is necessary.

There are 3 alternatives available to the clinician: to do a complete disarticulation at whatever level is indicated (34); to do the amputation at the lowest level possible with the idea in mind that a revision may be necessary; or to use a stump plug. The idea of a complete disarticulation, although quite tempting because of the assurance of no bony overgrowth, has the disadvantage of removing a member which is capable of supporting a prosthesis. In addition, another degree of motion is sacrificed. For these reasons the clinician usually chooses one of the two latter alternatives.

There has been a great deal of research on the use of intramedullary bone plugs made of silicone rubber. It was felt that a plug of this type would not only prevent stump overgrowth, but would also allow the patient to walk directly on the stump surface without the normal pain or skin breakdown because soft rubber would be capable of absorbing the greater part of the impace (25).

Research with Silastic 372 Medical-Grade Elastomer, produced by Dow Corning, has proved quite satisfactory (89). Early evaluation of thirteen below-knee amputations in which Silastic bone plugs were used suggest that stumps will be smoother, more pain free, and capable of tolerating increased end-bearing loads (89). A histological study of the effect of covering the bone stump has revealed no significant foreign body reaction (88) with the sili-

cone rubber plug encapsulated with a mesothelial-lined fibrous tissue without any sign of bursa formation. Further long range work is being done on silicone rubber bone plugs and results should be available in the near future.

Most clinicians choose to perform the amputation at the lowest level without the use of a plug because it is still the most reliable and most understood technique available.

Another bone abnormality which occurs in limb amputation is the occurrence of disuse osteoporosis, which is present when bone is not sufficiently stressed, especially in the aged and in stumps where prostheses are not worn (45,84,46). Disuse osteoporosis is associated with a diminished bone formation which does not keep up with the osteoclastic resorption. It is distinguished by an increase in the size of the medullary cavity, resorption of the cancellous bone and an overall thinning of the cortical bone with widespread presence of empty bone cell lacunae (45,78). The abnormally fragile bone can be treated by resumption of activity.

Many other problems, which are associated with the use of a prosthesis, are inherent in the basic design of all of today's protneses. For example, parts of the prosthesis which are not controlled by the stump are usually controlled by a system of mechanical controls actuated by various body movements. For instance, opening of a prosthetic hook on a below-elbow amputee is done by curling the shoulders to actuate a control wire. Associated with this is a very significant loss of energy and poor

cosmetic appearance. The body also has a limited number of control sites capable of operating these mechanical controls so that often an amputee loses some axis of motion. Further power loss occurs when forces are transmitted from the skeletal system through muscle and skin to the prosthesis' housing.

Many prostheses such as those for the hip and shoulder disarticulation must be held in place by a system of support straps. These are inefficient, uncomfortable and cosmetically undesireable.

A further inherent limitation in today's prostheses is a loss of feedback from the prosthetic device. Normally, control of the extremities' actions comes from a continuous force, velocity, and acceleration feedback to the brain. Following amputation, control of upper limb prostheses is based on continuous visual feedback which greatly limits the patient's efficiency.